Holocene salt-marsh sedimentary infilling and relative sea-level changes in West Brittany (France) using foraminifera-based transfer functions

Pierre Stéphan, Jérôme Goslin, Y. Pailler, Rose Manceau, Serge S. Suanez, Brigitte van Vliet-Lanoë, Alain Hénaff, Christophe Delacourt

BOREAS An international journal of Quaternary research

Holocene salt-marsh sedimentary infilling and relative sea-level changes in West Brittany (France) using foraminifera-based transfer functions

Journal:	*Boreas*
Manuscript ID:	BOR-093-2013.R3
Manuscript Type:	Original Article
Date Submitted by the Author:	14-Jun-2014
Complete List of Authors:	Stéphan, Pierre; IUEM, CNRS, laboratory LETG-Brest-Géomer, UMR 6554, Geography Goslin, Jérôme; IUEM, CNRS, laboratory LETG-Brest-Géomer, UMR 6554, Geography Pailler, Yvan; INRAP-Bretagne, Archaeology Manceau, Rose; CNRS, Laboratory LGP, UMR 8591, Physical Geography Suanez, Serge; IUEM, CNRS, laboratory LETG-Brest-Géomer, UMR 6554, Geography Van Vliet-Lanoë, Brigitte; IUEM, CNRS, Laboratory Domaines Océaniques, UMR 6538, Marine Geology Henaff, Alain; IUEM, CNRS, laboratory LETG-Brest-Géomer, UMR 6554, Geography Delacourt, Christophe; IUEM, CNRS, Laboratory Domaines Océaniques, UMR 6538, Marine Geology
Keywords:	Holocene, Sea-level change, France, Foraminifera, Transfer function, Salt-marsh

Holocene salt-marsh sedimentary infilling and relative sea-level changes in West Brittany (France) using foraminifera-based transfer functions

PIERRE STÉPHAN, JÉRÔME GOSLIN, YVAN PAILLER, ROSE MANCEAU, SERGE SUANEZ, BRIGITTE VAN VLIET-LANOË, ALAIN HÉNAFF AND CHRISTOPHE DELACOURT

Stéphan, P., Goslin, J., Pailler, Y., Manceau, R., Suanez, S., Van Vliet-Lanoë, B., Hénaff, A. & Delacourt, C.: Holocene salt-marsh sedimentary infilling and relative sea-level changes in West Brittany (France) using foraminifera-based transfer functions. *Boreas*...

In order to reconstruct the former sea-levels and to better characterize the history of Holocene salt-marsh sedimentary infillings in West Brittany (western France), local foraminifera-based transfer functions were developed using Weighted-Average-Partial-Least-Squares (WA-PLS) regression, based on a modern dataset of 26 and 51 surface samples obtained from salt-marshes in both the bay of Tressseny and the bay of Brest. Fifty cores were retrieved from Tresseny, Porzguen, Troaon and Arun salt-marshes, which were litho- and biostratigraphically analyzed in order to reconstruct palaeoenvironmental changes. A total of 26 AMS ^{14}C age determinations were performed within the sediment successions. The Holocene evolution of salt-marsh environments can be subdivided into four stages: (1) a development of brackish to freshwater marshes (from *c.* 6400 to 4500 cal. a BP); (2) salt-marsh formation behind gravel barriers in the bay of Brest (from 4500 to 2900 cal. a BP); (3) salt-marsh erosion and rapid changes of infilling dynamics due to the destruction of coastal barriers by storm events (*c.* 2900-2700 cal. a BP); (4) renewed salt-marsh deposition and small environmental changes (from 2700 cal. a BP to present). From the application of transfer functions to fossil assemblages, 14 new sea-level index points were obtained indicating a mean relative sea-level rise around 0.90±0.12 mm a^{-1} since 6300 cal. a BP.

Pierre Stéphan (pierre.stephan@univ-brest.fr), Jérôme Goslin, Serge Suanez, Alain Hénaff, IUEM, CNRS, laboratory LETG-Brest-Géomer, UMR 6554, France; Yvan Pailler, INRAP Bretagne, laboratory Trajectoires, UMR 8215 & laboratory LETG-Brest-Géomer, UMR 6554, France; Rose Manceau, CNRS, Laboratory LGP, UMR 8591, France; Brigitte Van Vliet-Lanoë, Christophe Delacourt, IUEM, CNRS, Laboratory Domaines Océaniques, UMR 6538, France; *received 31st October 2013, accepted 19th June 2014.*

During the last two decades, several reconstructions of late Holocene relative sea-level (RSL) change in the temperate zone have been developed using quantitative methodological approaches based on micro-fossil taxa such as foraminifera-based transfer functions (FBTFs). This statistical tool was widely used in the eastern north-Atlantic salt-marsh environments to produce high-resolution RSL reconstructions, notably along the coasts of UK (e.g. Edwards & Horton 2000, 2006; Horton *et al.* 2000; Edwards 2001; Gehrels *et al.* 2001; Horton & Edwards 2003, 2005; Boomer & Horton 2006; Massey *et al.* 2006; Barlow *et al.* 2013) and in the Bay of Biscay (Leorri *et al.* 2008a, b, 2010, 2011; Rossi *et al.* 2011). The strong correlation of agglutinated salt-marsh foraminiferal assemblages with elevation was used in the transfer function approach to quantify the relationship between faunal data (relative abundance of species) and environmental data (tide levels) by regression analyses. The modern relationship was then applied to cores to reconstructed former tide levels from fossil assemblages.

Despite the high performence of this quantitative approach, only a limited number of FBTFs was attemped from salt-marsh sedimentary infillings along the French coasts of the Atlantic and the English Channel (Horton & Edwards 2006; Leorri *et al.* 2008b, 2010; Rossi *et al.* 2011). In Brittany (western France), previous Holocene sea-level records are restricted to the Bay of Mont-Saint-Michel (marais de Dol) which are based on intercalated peat layers in the sediment succession (Van de Plassche 1991). On the north coast of Brittany, several peat deposits outcropping on the beaches of Saint-Marc and Brehec were studied by Ters (1986) and Delibrias *et al.* (1982). Similar deposits were

used by Giot (1969) and Morzadec-Kerfourn (1969) for Holocene RSL reconstructions on the north-west coast of Brittany. Recently, Goslin *et al.* (2013) provided some new data for the west Brittany from basal peat contacts recognized on several beaches at low tide. Nevertheless, such basal peat deposits only allow reconstruction of long-term RSL movements (Gehrels 1999) and are often absent for the late Holocene period. This can lead to discontinuous and poorly defined RSL reconstructions for the late Holocene period. In the south coast of Brittany, few sediment successions have been studied by palynological analyses (Visset *et al.* 1995; Gaudin 2004; Visset & Bernard 2006), yet no attention was given to the RSL changes. Only Rossi *et al.* (2011) developed a FBTF to reconstruct former RSLs for the last two centuries in the Morbihan Gulf.

Knowledge of coastal sedimentary infillings of Brittany is quite limited and has recently undergone geological investigations. Yet, these were mainly concentrated on the foreshore of major sedimentary coastal wedges, and on incised valley systems, delivering great information on the postglacial transgression of Brittany for the early to mid-Holocene periods (Billeaud *et al.* 2007, 2009; Sorrel *et al.* 2009, 2010; Tessier *et al.* 2010a, b). However, it must be noted that the stratigraphy of small salt-marsh environments has been quite poorly documented until now (Morzadec-Kerfourn 1969; Stephan 2011a). In a recent synthesis of data collected since the beginning of the 2000s on the French Atlantic coastal sediment wedges, Tessier *et al.* (2012) highlighted the strong control exerted by rapid climatic changes on the infilling dynamics. Periods of enhanced storminess that occurred during the Holocene were recognized within stratigraphies, and are responsible for significant morphological changes of coastlines.

The aim of this paper is to examine the late Holocene sedimentary successions of four salt-marshes of West Brittany, France, and to develop new and more accurate RSL reconstructions for the area. To achieve these aims, we developed local FBTFs in both the bay of Tresseny and Brest on the basis of the present-day distribution of foraminiferal-assemblages along cross-marsh transects. Moreover, salt-marsh sedimentary infillings are described using litho- and biostratigraphical analyses. Local FBTFs are applied to fossil foraminiferal-assemblages from vibracores to perform the palaeoenvironmental reconstructions. The results are used to develop 17 new Sea-Level Index Points (SLIPs) for West Brittany.

Regional setting and study areas

Study areas are located on the northwest coast of Brittany (Fig. 1). This area is part of the Armorican domain, located south-west of the English Channel, and was considered as a tectonically stable region during the Holocene (Ters 1986; Morzadec-Kerfourn 1995). The major deformation seems to be the result of the hydrostatic loading of the Channel platform during the Holocene transgression. A subsidence of 1.5 m of the coast of Finistère is expected over the last 6000 years (Lambeck 1997). Studied sites were selected because these areas present the thickest sediment successions with low energy sediments (fine sand, silt and clay), dateable organic deposits and an open connection to the sea.

Tresseny salt-marsh covers an area of 13 ha and is restricted to the inner part of a small macrotidal narrow bay (Fig. 2) forming the mouth of the Quillimadec coastal river. This bay is located on the northwest coast of Brittany, characterized by sand-dominated sedimentary environments, composed of sandflats in the lower foreshore, sandy beaches in the middle-upper foreshore and coastal dune barriers and spits isolating brackish marshes. The coast is mainly exposed to North to North-West Atlantic swells. The tidal range reaches up to 7.2 m on spring tides and 3.45 m on neap tides (Table 1). The bay has a total surface of 130 ha, a length of 3.2 km and a width ranging from 200 m in the inner part and 500 m in the outer part. However, the bay is significantly narrower in its central part where the width does not exceed 75 m, therefore sheltering the marsh from wave impact, especially its northern part. Tresseny marsh is mainly covered with halophytic plants: *Plantago maritima*, *Halimione portulacoides*, *Puccinellia Maritima*, *Juncus maritimus*. In the 17th century, the inner part of the Tresseny bay was transformed into meadows by a drainage system after the construction of a tide-mill.

The bay of Brest is approximately 11 km wide and 27 km long. The southern and northern parts of the bay are mainly composed of gravel beaches and unconsolidated cliffs formed by periglacial deposits; while the eastern part is composed of large mudflats and estuaries separated by rocky headlands. The bay is a fetch-limited environment, where bigger storm-waves never exceed 1 m

in height (Stéphan 2011b). The area is considered a macrotidal environment, with a tidal ranging from 5.9 m on spring tides and 2.8 m on neap tides (Table 1). On the east coast of the bay of Brest, the Lanveur marsh is located in the inner part of a large open bay sheltered by rocky headland. Vegetation cover forms a 100 m wide zone in the inner part of the bay (Fig. 2) composed of halophytic plants as *Puccinellia maritima*, *Halimione portulacoides* in the high marsh, and *Spartina alterniflora* in the low marsh. A large mudflat characterized by hierarchical tide channels represents the outer part of the bay. Others studied marshes in the bay of Brest (Porzguen, Troaon and Arun marshes) are back-barrier environments. Coastal barriers are composed of mixed sand and gravel material and present a single ridge affected by episodic overwash events (Stéphan 2011b, c). The marshes cover areas ranging from 3 ha for in both Porzguen and Arun salt-marshes and 6 ha for Troaon salt-marshes. The elevation of the surface corresponds to the mean high-water spring-tide level. The superficial sediment cover is a grey silty-clay mud (mean grain size between 20 and 40 μm). The bottom of tidal channel indicates higher mean grain size values (around 300 μm). Marsh vegetation exhibits a vertical zonation and can be sudivided into high marsh covered by *Halimione portulacoides*, *Puccinellia Maritima*, *Plantago maritima* and middle marsh covered by *Spartina alterniflora* and *Salicornia fragilis*. The inner part of the marsh is covered by brackish water vegetation consisting of *Phragmites australis*, *Scirpus maritimus* and *Juncus maritimus*.

Material and methods

Transfer functions construction

Surface sediment sampling strategy was based on cross-marsh transects, covering tidal flat (or channel) to brackish marsh, in order to cover different marsh subenvironments in terms of elevation relative to tidal levels. The top 10 cm of sediment was sampled, considering that infaunal populations of agglutinated foraminifera living at depths of up to 10 cm have been reported from salt-marshes in the French Atlantic coast (Duchemin *et al.* 2005) and also in the mid-Atlantic and southeastern USA (Goldstein *et al.* 1995; Saffert & Thomas 1998; Hippensteel *et al.* 2000). Consequently, a vertical

error of ±0.10 m was added to the palaeomarsh reconstructions performed by using transfert function models.

Topographic elevation was measured for all modern samples relative to the French ordonance datum (NGF) using a Trimble 5700/5800 Differential GPS. The total elevation error related to DGPS measurement (±0.02 m) and geodesic marker precision (±0.1m) is estimated to ±0.12 m (Suanez *et al.* 2008). Topographic elevations were converted to tide levels using measurements performed by the SHOM (Service hydrographique et Océanographique de la Marine). The margin of error related to the datum conversion was less than ±0.001m.

Modern samples were sieved through a 500 µm and 63 µm mesh and washed to remove clay and silt material. The residual fraction was split into 3 subsamples (<100 µm, 100-200 µm, >200 µm). Where possible, a minimum amount of 100 specimens of foraminifera (dead and alive) were counted for each subsample using a stereoscopic binocular microscope. Species identification was mainly based on specific papers showing modern assemblages and their distribution patterns in the French Atlantic salt-marshes (Moulinier 1996; Redois & Debenay 1996; Goubert 1997; Armynot du Châtelet *et al.* 2005; Duchemin *et al.* 2005; Debenay *et al.* 2006; Leorri *et al.* 2010; Rossi *et al.* 2011). *Ammonia* and *Elphidium* were recorded as generic groups (Hayward *et al.* 2004; Horton & Edwards 2006; Kemp *et al.* 2012).

A detrended canonical correspondance analysis (DCCA) was employed to determine if taxon-environment response was unimodal (Gaussian) or linear (Sejrup *et al.* 2004) using CANOCO 4.0 (Ter Braak & Smilauer 1998) software. Furthermore, the programme C2 (version 1.4, Juggins 2004) was used to construct the transfer functions. The performance of the transfer functions was assessed by calculating root mean squared error of prediction (RMSEP), maximum bias, and the correlation of observed versus predicted values (r^2). Data was jacknifed to assess the overall predictive abilities of the training set.

Stratigraphical analysis

The lithostratigraphy of sediment infilling was investigated via a series of 50 auger cores (Fig. 2). A set of vibracores were also collected (called "reference cores" in the paper) and separated into sections in the laboratory for AMS ^{14}C dating, sedimentological and foraminiferal analysis. The ground surface elevation was obtained for all cores by DGPS mesurements. Possible sources of altitudinal error have been considered in detail by Shennan (1986). Overall altitudinal error was evaluated to ±0.14 m, accounting for (i) a potential ±0.02 m incertitude in the measurement of the stratigraphic position of the sample and (ii) a ±0.12 m uncertainty due to levelling to the benchmark. Grain size analysis was conducted after a destruction of organic material using a laser analyzer (type Malvern Mastersizer 2000) for fine fraction (<1 mm) and by sieving procedure for coarse material (>1mm). 26 carbon-rich sediment samples were collected from reference cores and dated by radiocarbon, providing a reliable chronological framework of the salt-marshes sedimentary infillings (Table 2). The conventional radiocarbon dates were calibrated using software Calib 7.0 (Stuiver & Reimer 1993) and the IntCal13 calibration curve (Reimer *et al.* 2013). Errors in the inferred radiocarbon dates cannot be excluded because of the possible contamination of the sediment by older or younger carbon, such as by rootlet penetration or inwashed material. Nevertheless, most of radiocarbon measurements were carried out on detritial fragments of *in situ* halophitic plants selected under binocular microscope. Indeed, as pinpointed by several authors (Gehrels *et al.* 1996; Törnqvist *et al.* 1998; Gehrels 1999) the fragility of plants remains largely reduces their potential of re-deposition and the latter can thus be considered as reflecting the depositional environment of the dated sediment.

Results

Contemporary foraminireral distribution

Along Tresseny salt-marsh transect, 26 samples containing 14 species of foraminifera with an abundance of at least 2% in a single sample were collected between MHWNT and MHWST (Table S1). Fig. 3 exhibits the main foraminiferal species of the total (live and dead) training set plotted against the elevation. Only one sample contained less than 200 individuals. Hyaline and porcelanous

species were present only in samples collected in the tidal creek below 2.75 m NGF. Calcareous foraminiferal assemblages are dominated by *Haynesina germanica* (mean value and range: 44%, 0-73%) followed by *Elphidium* sp. (9%, 0-29%) and *Ammonia* sp. (8%, 0-18%). Species diversity decreases with increasing elevation along the transect. Agglutinated species dominate the assemblages in the upper part of the marsh. *Jadammina macrescens* (38%, 16-64%) and *Miliammina fusca* (34%, 16-52%), together with *Haplophragmoides wilberti* (25%, 15-42%) were the most abundant species between 2.75 m NGF and 3.62 m NGF.

At Lanveur, 23 samples were collected between the MTL and the MHWST (Fig. 3). Ten species of foraminifera (abundance ≥2% in a single sample) were identified (Table S1). Three main zones can be distinguished along the transect from foraminiferal assemblages corresponding to the mud-flat, the low salt-marsh and the high salt-marsh, respectively (Fig. 3). Calcareous species dominate the transect's lowest zone from 0.5 m NGF to 1 m NGF. Foraminifera in the mud-flat zone are dominated by *H. germanica* (44%, 22-65%), *Ammonia* sp. (41%, 31-57%) and *Elphidium* sp. (7%, 2-13%). The most abundant species found on the low salt-marsh zone was *M. fusca* (60%, 30-81%) at an elevation ranging from 1 m to 2 m NGF. *J. macrescens* (41%, 29-63%) dominates the high salt-marsh zone between 2 m NGF and 3.2 m NGF.

Along the Arun cross-marsh transect, a total of 30 samples were collected between the MHWNT and the HAT (Fig. 3). Foraminiferal assemblages present a low species diversity with only 5 agglutinated species of foraminifera with an abundance of at least 2% in a single sample identified. The most abundant species were *Trochammina inflata* (31%, 11-57%) and *J. macrescens* (27%, 5-69%), together with *M. fusca* (21%, 3-61%) and *H. wilberti* (20, 2-52%). Two upland samples fringing the salt-marsh contained no foraminifera (E29 and E30, Fig. 3).

Foraminifera-based transfer functions development

In the bay of Brest, we developed transfer functions to reconstruct palaeomarsh elevation for fossil samples using three models (Table 3). The first 'all data' model used the full modern dataset obtained from the two cross-marshes transects located in the Bay of Brest. The training set consisted of 51

modern surface samples and 14 species of foraminifera, covering an elevation range of 3.27 m. DCCA indicated that the modern species-environmental response was unimodal with a gradient length of 2.515 allowing us to apply WAPLS regression method. The model does not successfully predict the elevation of samples. The transfer function performance estimated a high RMSEP of ±0.48 m and a low r^2 at the 2nd component (Table 3). This suggests that the predictive abilities and the relationship between observed and predicted values are poor and therefore induce high associated errors (Fig. 4). When a large training set spans a long elevation range, some samples may present a weak relationship with elevation because of the possible influence of other environmental factors, taphonomic processes or natural variability in species response to their controlling variable (Edwards & Horton 2000; Edwards 2001; Woodroffe & Long 2009; Barlow *et al.* 2013). Consequently, some authors remove surface samples collected in tidal flats and low salt-marshes which often show non-linearity with elevation. This procedure aims to increase the transfer function's predictive ability (Edwards & Horton 2000; Hamilton & Shennan 2005). In the 'all data' model, mudflat samples are derived from Lanveur cross-marsh transect (Fig. 4) where a sharp transition is observed between the unvegetated mudflat zone dominated by calcareous taxa and the vegetated saltmarsh zone dominated by agglutinated species (Fig. 3). The samples from these two different foraminiferal zones are clearly separated in the plot of observed versus predicted elevation, which illustrates the difficulty to combine both in the same regression model. However, samples collected in the salt-marsh zone seem to be in alignment according to the elevation range. Therefore, a second 'salt-marsh' model was developed after excluding samples from mudflat environment. This reduced the training set to 43 samples and 9 taxa. The elevation range was shortened to 2.58 m.

The 'salt marsh' model in comparison with the 'all data' model failed to produce a better performance (Table 3) on account of the large number of samples with high residual values. Two outliers were represented by samples L10 and L19 collected along the Lanveur cross-marsh transect which exhibited an unusually high abundance of *Ammonia* sp. and *Elphidium* sp. compared to other neighbouring samples (Fig. 4). Furthermore, 10 samples collected both in the salt-pans and tidal creeks of the Arun salt-marsh seemed to have a poorly defined relationship to elevation. This likely suggested the influence of other environmental factors within these microforms. The salt-pans and

tidal-creeks are characterized by the absence of a vegetation cover and probably by large variations of temperature and salinity that may disturb locally the general pattern of the foraminiferal zonation. These samples were removed from the training set to develop a third 'pruned' salt-marsh model using WAPLS regression method. This model consists of 29 modern surface samples, 8 foraminifera taxa and cover an elevation range of 2.35 m. The transfer function performance estimates a RMSEP of ±0.20 m and a r^2 of 0.94 at the component 3 (Table 3). This suggests that the predictive abilities and the relationship between observed and predicted values were significantly improved. However, a part of this performance improvement can be considered as artificial. By excluding samples from the training set, we reduced the size of the modern dataset and we made the choice not to capture the entire diversity of the sampled modern environments. This approach has automatically lead to a better performance of models, but it limits their ability to reconstruct all the past environments.

For the Tresseny salt-marsh, we developed a model ('Tresseny model') using the entire training set collected along the cross-marsh transects. This model included all modern samples collected and all species and constist of 26 modern surface samples, 14 foraminifera taxa, covering an elevation range of 1.61 m. DCCA suggests that unimodal methods of regression and calibration were appropriate because the gradient lengths were greater than 2. The Weighted Averaging-Partial Least Squares method was used to produce a model with a RMSEP of ±0.14 m and a r^2 of 0.90 at the 2nd WAPLS component. The fit between observed and predicted elevation is good, albeit there are some non-linearities by places along the elevation range (Fig. 5). Samples collected on the unvegetated surface of the tidal creek show a poor statistical relationship with elevation. This is probably due to the influence of other environmental factors or taphonomic processes (Edwards & Horton 2000) previously described.

Salt-marshes sedimentary infilling: lithostratigraphy, biostratigraphy

Based on sedimentological analyses (grain size analysis, sedimentary structures, organic and foraminiferal contents), the investigated Holocene sediment successions were subdivided into 9 lithofacies (LF1 to LF10, Table 4). Their interpretation in terms of depositional environments were

based on classic models (Reineck & Singh 1980; Allen 2000, 2003), regional studies of estuarine and coastal areas (Billeaud *et al.* 2007, 2009; Lespez *et al.* 2010; Stéphan 2011a, b; Tessier *et al.* 2012; Goslin 2014), and comparison with modern sediments that characterize coastal environments in NW Brittany (Hallégouët 1971; Guilcher *et al.* 1990) and the bay of Brest (Stéphan 2011a).

At Porzguen, a basal peat unit (LF1) overlays a weathered shale pre-Holocene surface (Fig. 6). The age of this unit is dated to 5605-5324 cal. a BP at the base and 5036-4625 cal. a BP at the top. Benthic foraminifera assemblages are dominated by *T. inflata* (average 35%), *J. macrescens* (average 30%) and *H. wilberti* (average 30%, Table S2). This assemblage is indicative of high marsh environment. The basal peat unit is overlaid by an organic silty clay unit (LF2) found from -0.65 to +1.1 m NGF in core P-C2. The contact between the basal peat and this overlaying unit is gradational and reflects an increase of the marine influence in a salt-marsh environment probably sheltered by a coastal barrier. From +1.1 to +3 m NGF, this unit is replaced by a grey silty-clay (LF4) characterized by two 20 cm thick layers with milimetric laminations of black organic-rich silt found at a depth between +1.4 m NGF and +2.2 m NGF. This unit presents foraminiferal populations highly dominated by *T. inflata* (Fig. 7A). However, the laminated layers show no foraminifera and may have accumulated under low salinity conditions, in a back-barrier freshwater pond during phases of salt-marsh closure by the gravel barrier. At Porzguen, the top unit of the sedimentary succession at Porzguen corresponds to LF2. Fossil foraminiferal assemblages are dominated by *T. inflata* (average 60%) and *J. macresens* (average 30%).

At Troaon, the holocene sediment inflilling is 5.5 m thick (Fig. 6). The base of the succession consists of reed peat layer containing phragmites macro-remains (LF1) and agglutinated foraminiferal populations dominated by *T. inflata*, *J. macrescens* and *H. wilberti* indicative of high marsh environment (Table S3). The timing of the peat deposition is between 6399-6015 and 4956-4569 cal. a BP. This deposit was found at a depth between -2.8 m NGF and -0.65 m NGF, which probably extends seaward and is overlaid by the gravel barrier and beach. Overlaying the peat is a silty clay sediment with salt-marsh plant fragments and rootlets (LF2) found from -2 m NGF to the present-day surface. It forms a gradual transition into the underlying basal peat unit. Benthic foraminifera assemblages are dominated by *J. macrescens* and *T. inflata* in relatively equal proportion (about 45%) indicative of

high marsh environment (Fig. 7B). Two 10 cm thick layers of silty-sand horizons (LF3) were found between +0.1 and +0.7 m NGF in cores T-C1 and T-C2. The contact between these horizons and the clay unit is very sharp, which indicates erosion. These horizons are characterized by numerous shell fragments and the significant presence of hyaline species as *H. germanica* and *Elphidium* sp. indicative of a low marsh environment.

At Arun, the Holocene succession is composed of two main lithofacies (LF2 and LF3), characterized by interbedded coarse deposits (LF5) in the seaward cores which are associated with several phases of gravel barrier construction and breakdown (Fig. 6). A silty sand unit forms the base of the sequence. This unit is found between -0.2 and +0.7 m NGF in the seaward cores A-C10 (Fig. 7C). Associated with abundant organic detrital remains, foraminifera assemblages are dominated by *J. macrescens* (average 55%) and *T. inflata* (average 40%, Tables S4, S5) indicating a high-marsh environment (Fig. 7D). We interpret the presence of *M. fusca* and some calcareous species, in association with shell fragments, as the expression of an open-bay environment where waves convey material from the low-marsh to foreshore domains. Two dates indicated that this unit was formed between 2941-2748 and 2691-2159 cal. a BP. From +0.7 m NGF to the present-day surface, a silty clay unit is 2.9 m thick formed from 2690-2160 cal. a BP. Foraminifera assemblages are dominated by *J. macrescens* (average 48%) and *T. inflata* (average 45%) indicative of a high-marsh environment. In core A-C10, an interbedded coarse sand and gravel deposit corresponding to LF5 is found at an elevation between 1.7 and 2.5 m NGF (Fig. 7C). This deposit may correspond to a second overwash fan due to the opening of a breach within the coastal barrier.

In the bay of Tresseny, the base of the succession consists of well-humified basal peat (LF6) covering a weathered granite substrate on a mean thickness of 1 to 1.5 m (Figs 8, 9). The significant proportion of sand and the absence of foraminifera seems to indicate a back dune brackish marsh. A series of dates from core G-C2 indicate this basal peat was formed from 6403-6299 cal. a BP in this core. The age of the upper part of the basal peat range from 4826-4572 cal. a BP. A coarse sand unit (LF7) overlies the basal peat at a depth of -2.2 m NGF up to the most landward cores at a depth of +1 m NGF, with a thickness gradually decreasing to 0.10 m at core G-C5. The sharp transition between LF6 and LF7 suggests a rapid change toward high hydrodynamic conditions. The age of this

environmental change is known by a series of 5 radiocarbon dates obtained on the minerogenic sandy-silt unit (LF8) overlying the coarse sand layer. The ages cover a short period around 2850-2700 cal. a BP and suggest high rates of sedimentation (around 12 mm a^{-1}). Foraminiferal analysis from core G-C2 indicates low density of specimens, probably reworked and composed by agglutinated species such as *J. macrescens*, *H. wiberti*, *T. inflata* and *M. fusca*. The scarcity of foraminifera is probably due to a dilution of specimens related to the high rates of sedimentation. Associated with the low density of detrital plant fragments, this suggests a sand-flat environment subjected to relatively high hydrodynamic conditions and high sediment supply (Goslin *et al.* 2013). The upper part of the succession is formed by an organic-rich fine sand unit (LF9) within the seaward cores and reed peat (LF6) in the landward cores. This unit is found from +2.8 m NGF to the present-day surface. Foraminifera assemblages are dominated by *J. macrescens* (average 55%), *H. wiberti* (average 22%) and *M. fusca* (average 16%) (Fig. 9, Table S6). It reflects a gradual change from a sand flat to a salt-marsh between 1825-1631 and 527-338 cal. a BP.

Discussion

Application of transfer function models to fossil sediment successions

At Tresseny, the palaeomarsh elevation reconstructions are based on the application of the 'Tresseny Model' with a low RMSEP value (±0.14 m). In the bay of Brest, the 'pruned' salt-marsh model was prefered because it presents the lowest RMSEP values (±0.20 m) compared to other developed models for this area (Table 3). The levels of precision are comparable to those found within the same tidal range around the northeast Atlantic coasts (Horton & Edwards 2006; Gehrels *et al.* 2001; Massey *et al.* 2006; Leorri *et al.* 2008a, b, 2011). In Brittany, Rossi *et al.* (2011) developed a model with a lower RMSEP value of ±0.10 m within the mesotidal setting of the Morbihan Gulf (tidal range *c.* 3 m at spring tide).

To explore the applicability of these transfer models to our fossil sedimentary successions, we use the minimum dissimilarity coefficient (MinDC) measure within the modern analogue technique

(MAT) (Birks 1995). The 20th percentile of the dissimilarity coefficients calculated between all modern samples was used as the cut-off between 'close' and 'poor' modern analogues for fossil samples. The 5th percentile was the threshold for defining 'good' modern analogues (Barlow *et al.* 2013; Watcham *et al.* 2013).

At Tresseny, foraminiferal occurence is only significant at 95 cm depth. The assemblages are dominated by *J. macrescens* (average 55%), *H. wiberti* (average 22%) and *M. fusca* (average 16%). The palaeoelevations of the marsh provided by the transfer function reconstructions are around the MHWST level, ranging from +3.5 m to +3.95 m NGF (Fig. 9, Table S6). With the exception of one fossil sample, the MAT identifies a majority of 'good' and 'close' analogues therefore indicating these results to be reliable. The much higher abundance of the foraminiferal populations associated with the increase of the organic content in the upper part of the sediment core seems to reflect a gradual change from a sand flat to a salt-marsh between 1820-1690 cal. a BP and the present-day (accretion rate around 0.6 mm a^{-1}).

At Porzguen, the transfer function reconstructions indicate a palaeomarsh surface elevation between +3 and +4 m NGF (Fig. 7A, Table S2) corresponding to a high salt-marsh environment. A significant number of fossil samples have 'poor' modern analogues, especially in the upper part of the sediment succession corresponding to LSU4. Based on lithostratigraphical analysis, this deposit is interpreted as a brackish marsh episodically transformed into a freshwater swamp occupying a back-barrier pond. A possible explanation of the 'unreliable' results obtained by FBTF is the absence of samples corresponding to this particular depositional environment in our modern training set. In this case, the model does not provide a good approximation of past environments. Furthermore, fossil samples with 'poor' analogues are characterized by a very high proportion of *T. inflata* within assemblages (Fig. 7A). The high representation of this robust species may result from a preferential enrichment of the fossil assemblages due to taphonomic processes affecting the other species and biassing the interpretations (Alve & Murray 1994; Goldstein & Watkins 1999; Patterson *et al.* 1999; Horton & Edwards 2006).

A similar interpretation could explain the few 'close' analogues within the basal peat unit (LF1) at Troaon (Fig. 7B, Table S3). The FBTF reconstruction based on 'close' analogues suggests a

palaeomarsh elevation between +3.26 and +3.67 m NGF for this deposit. Within the two silty-sand layers corresponding to LF3, quantitative reconstructions indicate major changes of palaeomarsh elevations. Despite 'poor' modern analogues of fossil samples, the estimations provided by the pruned 'salt-marsh' model are of -0.82 and -0.49 m NGF for both the lower and upper horizon, respectively. These elevations correspond to tide levels ranging from the MLWNT to the MT. These layers are associated with erosional contacts and probably reflect sediment inputs from the foreshore during an opening period of salt-marsh environment caused by coastal barrier breakdown. The upper part of the sediment succession (LF6) shows reconstructed palaeosurface elevations between +2.81 and +3.74 m NGF indicative of an accretionary environment under a RSL rise trend.

At Arun, the reconstructed palaeomarsh elevation is between +2.39 and +3.54 m NGF (Tables S4, S5) corresponding to tide levels between the MHWNT and the MHWST (Figs 9, 10). The number of 'poor' fossil analogues is significant within core A-C14, resulting from high proportion of *T. inflata* in foraminiferal assemblages, probably reflecting brackish marsh conditions during closure of salt-marsh. Throughout the cores A-C10 and A-C14, the low amplitude fluctuations in the reconstructions may be related to the gravel barrier evolution (episodic breaching or overwash), leading to temporary changes in the hydrodynamic conditions (wave and tide), vegetation cover and foraminiferal zonation in the protected back-barrier setting.

New SLIPs from West Brittany and comparison with existing Holocene RSL records

In this section we initially convert the results of FBTFs models into new RSL records for West Brittany (Table 2) and subsequently compare them with previously obtained similar data (Table 5), produced along the Brittany coastline (Morzadec-Kerfourn 1969; Van de Plassche 1991; Visset *et al.* 1995; Regnauld *et al.* 1996; Gaudin 2004; Visset & Bernard 2006; Stéphan & Laforge 2013; Goslin *et al.* 2013). The vertical position of the sea-level index point (SLIP) relative to present tide levels is calculated as (Shennan 1986; Van de Plassche 1986):

$$SLIP = H - D - I + C + A \quad (1)$$

where H is the height of the top core, D is the depth of the sample, I is the heigh of the deposition of the sample (indicative meaning), C is the core compaction, and A is the autocompaction (loss of porosity due to the load of overlying sediments). This latter parametter strongly affects the calculation of the SLIP position, especially for samples from unconsolidated peat successions (Gehrels 1999), yet is particularly hard to estimate (Allen 1999, 2000; Long *et al.* 2006; Edwards 2006; Massey *et al.* 2006, 2008). Consequently, most of Holocene sea-level studies focus mainly on basal samples to infer compaction effects (e.g. Denys & Baeteman 1995; Van de Plassche 1995; Gehrels 1999; Shennan & Horton 2002; Berendsen 2007) and consider the intercalated SLIP simply as an approximation.

From the 26 AMS ^{14}C dates obtained in this study, 12 were used to produce SLIPs with a indicative meaning defined by the palaeomarsh surface elevation reconstructed by the FBTFs models (Fig. 10). Two dates obtained at the base of the basal brackish peat of Tresseny were also used as basal SLIPs, assuming an indicative meaning ranging from the HAT to the MHWNT (Goslin *et al.* 2013). Results indicate a rise of the RSL around 5.5 m during the last 6300 cal. a within the northwest coasts of Brittany. The mean rate of RSL rise calculated by a linear regression with all SLIPs ($r^2 = 0.97$) is of 0.90±0.12 mm a^{-1} for the entire period.

A comparison between SLIPs produced in this study and previous RSL data obtained from Brittany is presented in Fig. 10. Most of previous data were converted into SLIPs using the same methodological approach as Leorri *et al.* (2012). We use the indicative meaning reported in original publications. Local tide ranges used for coastal sites are presented in Table 1 and details about SLIPs produced are given in Table 4. Radiocarbon dates were also calibrated using the IntCal13 calibration curve (Reimer *et al.* 2013) to allow comparisons with our results. Fig. 10 illustrates that the SLIPs produced in this paper are consistent with previous RSL records and improve precision from c.6500 cal. a BP. Despite the wide incertitude boxes drawn for the previous data, a vertical variability between the SLIP is visually observed between the sites located at the SE part of Brittany and the points obtained in the NE and NW parts of Brittany. Lambeck (1997), followed by Leorri *et al.* (2012) highlighted the evident north-south trend in the Hococene sea-level rise in the Gulf of Biscay, mainly due to the ice-induced signal (glacio-isostacy) producing a relatively long-wavelength pattern with a

dominant north/south gradient. However, according to Leorri *et al.* (2012), the ocean-induced signal (hydro-isostacy) produces spatial gradients that are perpendicular to the shoreline, due to the geometry of the ocean loading. As a peninsula, Brittany appears to be an appropriate area to study the ocean-induced signal in detail. However, exploring this question along the coast of Brittany remains difficult in the state of our knowledge because of the lack of available basal SLIPs (only 10) providing reliable altitudinal sea-level data, notably in the eastern part of Brittany.

Salt-marshes evolution

Based on the lithostratigraphical and biostratigraphical analyses, a general pattern of Holocene salt-marsh evolution subdivided into four stages is proposed for West Britanny.

Stage 1: Basal peat formation (6400 to 4500 cal. a BP). - From 6400 to 4500 cal. a BP, extensive *Phragmites* marshes were formed around the present-day shoreline position. They expanded laterally and vertically under the influence of a rising water table until they reached an elevation of about 0 m NGF or more. In Tresseny salt-marsh, only scarce foraminifera were present in the basal peat, reflecting freshwater or brackish conditions. During this first stage of sedimentary infilling, the bay of Tresseny was probably separated from the sea by the presence of a wide coastal dune barrier located further seaward. In the bay of Brest, *Phragmites* macro-remains were not encountered and high-marsh foraminifera species such as *J. macrescens* and *T. inflata* were broadly present in the basal peat units. This reflects the influence of the tide in a high salt-marsh environment. Our results are consistent with those obtained by Morzadec-Kerfourn (1975) and more recently by Goslin *et al.* (2013) on the northern and southern coasts of the Finistère region: the base of a brackish basal peat found on the Vougot beach (Fig. 1) at an elevation of -3.52 m NGF gave an age of 6880 cal. a BP, while a similar deposit found at Tariec beach was dated around 6850 cal. a BP at an elevation of -3.80 m NGF (Goslin *et al.* 2013). In a general manner, it indicates that the formation of extensive reed and/or brackish marshes began around 6900 cal. a BP in places within the northwestern part of Brittany, under the joint influence of rising water table and stabilization of barrier systems on the foreshore. These

deposits are also associated with the presence of numerous coastal archaeological remains (megalithic gallery graves and menhirs) attributed to the neolithic period such as the gallery grave of Lerret, located 500 m seaward from Tresseny salt-marsh and dated about 4800-5000 cal. a BP.

Stage 2: Formation of backbarrier salt-marshes (4500 to 2900-2700 cal. a BP). - Over the basal peats, an accumulation of clayey peat deposits indicates salt-marsh expansion from 4500 cal. a BP, probably behind gravelly or sandy barriers offering sheltered conditions for high-marsh development. In the sediment successions of the bay of Brest, the transition from basal peat is gradual and the reconstructed palaeosurfaces are around the MHWST. At Tresseny, deposits corresponding to this stage were not preserved; however it is possible that brackish conditions were maintained behind a large coastal dune barrier.

Stage 3: Deep reorganization of back-barrier sedimentary wedges (2900-2700 cal. a BP). - Around 2900-2700 cal. a BP, the sediment successions reveal that coastal sedimentary systems underwent deep modifications. At Tresseny, this stage corresponded to the erosion of the top of the basal peat layer and the deposition of a coarse sand layer, overlayed by a silty-sand deposit. In the bay of Brest, Troaon and Arun marshes revealed layers of silty-sand deposits corresponding to this period at an average elevation of around 0 to +1 m NGF. At Troaon, these layers contain shell fragments and rest unconformably over the high-marsh clayey peat. The dominance of hyaline species such as *H. germanica* and *Elphidium* sp. indicates a low salt-marsh depositional environment estimated around the MTL by the transfer function. Conversely, the Porzguen marsh revealed no discontinuities within the sedimentary succession, most likely due to its sheltered location.

At the scale of northwest Europe, the period around 3000 cal. a BP has been widely recognized as a period of climate deterioration (Van Geel *et al.* 1996; Barber *et al.* 2003, 2004; Magny 2004; Dark 2006; Gandouin *et al*. 2009; Charman 2010; Swindles *et al.* 2013; Tisdall *et al.* 2013), characterized by colder and wetter climatic conditions, with increased rainfall and largely enhanced storminess (Van Geel *et al.* 1996; Clark & Rendell 2009). Major disruptions of coastal sedimentary environments were also identified all along the European coasts, either in the English Channel region

(Long & Hughes 1995; Billeaud *et al.* 2009; Sorrel *et al.* 2009; Lespez *et al.* 2010; Tessier *et al.* 2012) or along the Atlantic coasts (Pontee *et al.* 1998; Tastet & Pontee 1998; Clavé *et al.* 2001; Moura *et al.* 2007; Sorrel *et al.* 2009). Archaeological remains suggest less dense settlement patterns at the end of the Late Bronze Age (Coquillas 2001; Pailler *et al.* 2011; Stéphan *et al.* 2013) and for several settlements abandonment, notably due to an important eolian activity within the northwest Europe coastal areas (Guilcher & Hallégouët 1991; Tisdall *et al.* 2013).

Hence, we explain the genesis of these erosive contacts and sedimentary hiatus by high-energy conditions having taking place around 3000 cal. a BP, either caused by storm events, reorganization of the back-barrier marsh drainage systems, or under the joint influence of both dynamics. We believe that several morphogenetic scenarios can be invoked:

(i) Severe storms could have caused major breaches in the barrier systems, erosion of back-barrier sedimentary succession and deposition of mixed material displaced from the foreshore domain (deposits of "Chenier" type). This scenario well suits the sedimentary succession of the Arun marsh, but appears largely unconvincing for the inner-estuary Tresseny marsh and so cannot be considered as regionally valid.

(ii) The terrigenous sand layer on top of the unconformity in the Tresseny succession likely reveals the onset of inner-estuary conditions around 3000 cal. a BP. At this period, coastal streams valleys may have been widened to answer the waterflow increasements that followed the onset of wetter conditions in the context of (i) considerably reduced slopes of the streams-flows due to deeper intrusions of the salt-wedges and (ii) important terrigenous infillings in the lower valley systems induced by the massive clearings that took place during the Iron age (Dark 2006).

(iii) Third, barrier breaching may have fostered the catchment of the tidal channels within the marshes and in turn induced an erosion of the sedimentary successions. Tidal flows within the marshes may have gained volume in response to barrier-breachings (Wang *et al.* 2000; Picado *et al.* 2013) and in turn, resulted in the incision of tidal channels as it was shown by Cleveringa (2000).

These morphodynamic processes are of primary importance as soon as RSL reconstruction is concerned. In fact, as proposed by Goslin *et al.* (2013), high morphogenic events could have artificially created accommodation space, subsequently infilled by sedimentary deposits of doubtful

origin. Thus, we consider that large uncertaintities remaining on the representativeness of the *c.* 2800 cal. a BP points we obtained within the Arun and Tresseny successions.

Stage 4: Formation of new salt-marshes (2700 cal. a BP to present). - A return of the high salt-marsh environment, after the deposition of the silty-sand units is reflected by foraminiferal assemblages dominated by *J. macrescens* and *T. inflata*. Gravel barriers of Troaon and Arun were rebuilt in front of the salt-marshes, gradually accreting until today. At Arun, two washover deposits were recognized throughout the sediment succession, probably related to episodic landward retreat of the gravel spit during storms. However, contrary to the 2900-2700 cal. a BP period, no major and synchronous phases of erosion were observed in the succession we studied. In the inner part of the bay of Tresseny, the formation of the salt-marsh began around 1820-1690 cal. a BP with the gradual colonization of the sand-flat environment by halophitic plants and the abundance of agglutinated foraminifera.

Conclusions

In order to improve the reconstructions of relative sea-level changes for the late Holocene period in Brittany (western France), foraminifera-based transfer functions were developed using total assemblages from 77 samples collected along three cross-marsh transects located in two coastal bays (bay of Brest and the bay of Tresseny) in the most western part of Brittany. In the bay of Tresseny, we used the whole training set (all samples and all species) to produce a WAPLS model with a RMSEP of ±0.14 m and r^2 of 0.90. In the bay of Brest, three models were successively developped by removing modern samples from mudflat, followed by tidal creeks and salt-pans in order to increase the transfer function's predictive ability. The resulting final WAPLS model has a RMSEP of ±0.20 m and r^2 of 0.94.

The mid- to late Holocene stratigraphy of four salt-marshes developed over the past 6500 cal. a BP in the bay of Brest and in the bay of Tresseny was studied by litho- and biostratigraphical analyses. These investigations give, for the first time, a chronological pattern of Holocene infill of small salt-marshes in western France. Sediment successions show (i) basal peat units indicating

extensive reed marshes between 6400 and 4500 cal. a BP, (ii) clayey peat deposits dominated by high-marsh foraminiferal assemblages corresponding to the expansion of salt-marshes into backbarrier environments between 4500 and 3600 cal. a BP, (iii) storm-induced deposits around 2900-2700 cal. a BP represented by a coarse sand layer in the Tresseny sediment succession, and by silty-sand layers containing shell fragments and hyaline species such as *H. germanica* and *Elphidium* sp. in the bay of Brest sediment successions and (iv) a return of high salt-marsh environment since 2700 cal. a BP, reflected by foraminiferal assemblages dominated by *J. macrescens* and *T. inflata*.

The application of transfer function models to fossil assemblages produced 14 new sea-level index points showing a relative sea-level rise of 5.5±0.5 m during the last 6300 years, at a mean rate of 0.90±0.12 mm a^{-1}. New data obtained in this study improve the vertical definition of the Holocene relative sea-level history along the coasts of West Brittany and convey new information on the late Holocene period. Nonetheless, further research is still required (i) to achieve a better understanding of the behavior of the sedimentary systems in the context of descelerating RSL rise, (ii) to better constrain the history of the last c. 3000 years and (iii) to estimate the influence of the hydro-isostatic signal on the Holocene trends of the RSL rise along the western coasts of France.

Acknowledgements.- This work is a contribution to the Archaeological Program of Molene Archipelago (funded by Regional Service of Archaeology of Brittany) and to the ANR program "Cocorisco" (French National Research Agency program for coastal risks assessment and management, ANR 2010-CEPL-001-01, Pôle-mer Bretagne). Special aknowledgements are given to Nicolas Gudicelli for field assistance and Elaine Harkin for her help in proof-reading the article. The authors acknowledge N. Barlow and an anonymous reviewer for their constructive remarks.

References

Allen, J.R.L. 1999: Geological impacts on coastal wetland landscape: some general effect of sediment autocompaction in the Holocene of northwest Europe. *The Holocene 1*, 1-12.

Allen, J.R.L. 2000: Holocene coastal lowlands in NW Europe: autocompaction and the uncertain ground. *In* Pye, K. & Allen, J.R.L. (eds.): *Coastal and Estuarine Environments: sedimentology, geomorphology and geoarchaeology*, 239-252. *Geological Society, London, Special Publication 175*.

Allen, J.R.L. 2003: An eclectic morphostratigraphic model for the sedimentary response to Holocene sea-level rise in northwest Europe. *Sedimentary Geology 161*, 31-54.

Alve, E. & Murray, J.W. 1994: Ecology and taphonomy of benthic foraminifera in a temperate mesotidal inlet. *Journal of Foraminiferal Research 24*, 18-27.

Armynot du Châtelet, E., Debenay, J.-P., Degré, D. & Sauriau, P.-G. 2005: Utilisation des foraminifères benthiques comme indicateurs de paléo-niveaux marins? Etude du cas de l'anse de l'Aiguillon. *Comptes Rendus Palévol 4*, 209-223.

Barber, K.E., Chambers, F.M. & Maddy, D. 2003: Holocene palaeoclimates from peat stratigraphy: macrofossil proxy climate records from three oceanic raised bogs in England and Ireland. *Quaternary Science Reviews 22*, 521-539.

Barber K.E., Chambers F.M. & Maddy D. 2004: Late Holocene climatic history of northern Germany and Denmark: peat macrofossil investigations at Dosenmoor, Schleswig-Holstein, and Svanemose, Jutland. *Boreas 33*, 132-144.

Barlow, N.L.M., Shennan, I., Long, A.J., Gehrels, W.R., Saher, M.H., Woodroffe, S.A. & Hillier, C. 2013: Salt marshes as late Holocene tide gauges. *Global and Planetary Change 106*, 90-110.

Berendsen, H.J.A., Makaske, B., Van de Plassche, O., Van Ree, M.H.M., Das, S., Van Dongen, M., Ploumen, S. & Schoenmakers, W. 2007: New groundwater-level rise data from the Rhine-Meuse delta

–implications for the reconstruction of Holocene relative mean sea-level rise and differential land-level movements. *Netherlands Journal of Geosciences 86*, 333-354.

Billeaud, I., Tessier, B., Lesueur, P. & Caline, B. 2007: Preservation potential of highstand coastal sedimentary bodies in a macrotidal basin: Example from the Bay of Mont-Saint-Michel, NW France. *Sedimentary Geology 202*, 754–775.

Billeaud, I., Tessier, B. & Lesueur, P. 2009: Impacts of Late Holocene rapid climate changes as recorded in a macrotidal coastal setting (Mont-Saint-Michel Bay, France). *Geology 37*, 1031–1034.

Birks, H.J.B. 1995: Quantitative paleoenvironmental reconstructions. *In* Maddy, D. & Brew, J.S. (eds.): *Statistical Modelling of Quaternary Science Data, Technical Guide 5*, 161-254. Quaternary Research Association, Cambridge.

Boomer, I. & Horton, B.P. 2006: Holocene relative sea-level movements along the North Norfolk Coast, UK. *Palaeogeography, Palaeoclimatology, Palaeoecology 230*, 32-51.

Charman, D.J. 2010: Centennial climate variability in the British Isles during the mid–late Holocene. *Quaternary Science Reviews 29*, 1539-1554.

Clarke, M.L. & Rendell, H.M. 2009: The impact of North Atlantic storminess on western European coasts: A review. *Quaternary International 195*, 31-41.

Clavé, B., Massé, L., Carbonel, P. & Tastet, J.-P. 2001: Holocene coastal changes and infilling of the La Perroche marsh (French Atlantic coast). *Oceanologica Acta 24*, 377-89.

Cleveringa, J. 2000: *Reconstruction and modelling of Holocene coastal evolution of the western Netherlands*. Ph.D. thesis, University of Utrecht, 198 pp.

Coquillas, D. 2001: *Les rivages de l'estuaire de la Gironde du Néolithique au Moyen Age*. Ph.D. thesis, University of Bordeaux, 1296 pp.

Dark, P. 2006: Climate deterioration and land-use change in the first millennium BC: perspectives from the British palynological record. *Journal of Archaeological Science 33*, 1381-1395.

Debenay, J.-P., Bicchi, E., Goubert, E. & Armynot du Châtelet, E. 2006: Spatio-temporal distribution of benthic foraminifera in relation to estuarine dynamics (Vie estuary, Vendée, W France). *Estuarine, Coastal and Shelf Science 67*, 181-197.

Delibrias, G., Guillier, M.T. & Labeyrie, J. 1982: Gif natural radiocarbon measurements IX. *Radiocarbon 24*, 291-343.

Denys, L. & Baeteman, C. 1995: Holocene evolution of relative sea level and local mean high water spring tides in Belgium - a first assessment. *Marine Geology 124*, 1-19.

Duchemin, G., Jorissen, F.J., Redois, F. & Debenay, J.-P. 2005: Foraminiferal microhabitats in a high marsh: consequences for reconstructing past sea levels. *Palaeogeography, Palaeoclimatology, Palaeoecology 226*, 167-185.

Edwards, R.J. 2001: Mid- to late Holocene relative sea-level change in Poole Harbour, southern England. *Journal of Quaternary Science 16*, 221-235.

Edwards, R.J. & Horton, B.P. 2000: Reconstructing relative sea-level change using UK salt-marsh foraminifera. *Marine Geology 169*, 41-56.

Edwards, R.J. & Horton, B.P. 2006: Developing detailed records of relative sea-level change using a foraminiferal transfer function: an example from North Norfolk, UK. *Philosophical Transactions of the Royal Society 364*, 973-991.

Edwards, R.J. 2006: Mid- to late-Holocene relative sea-level change in southwest Britain and the influence of sediment compaction. *The Holocene 16*, 575-587.

Gandouin, E., Ponel, P., Andrieu-Ponel, V., Guiter, F., de Beaulieu, J.L., Djamali, M., Franquet, E., Van Vliet-Lanoë, B., Alvitre, M., Meurisse, M., Brocandel, M. & Brulhet, J. 2009: 10,000 years of vegetation history of the Aa palaeoestuary, St-Omer Basin, northern France. *Review of Palaeobotany and Palynology 156*, 307-318.

Gaudin, L. 2004: *Transformations spatio-temporelles de la végétation du nord-ouest de la France depuis la fin de la dernière glaciation. Reconstitutions paléo-paysagères*. Ph.D.thesis, University of Rennes 1, 762 pp.

Gehrels, W.R. 1999: Middle and late Holocene sea-level changes in eastern Maine reconstructed from foraminiferal saltmarsh stratigraphy and AMS 14C dates on basal peat. *Quaternary Research 52*, 350-359.

Gehrels, W.R., Belknap, D.F. & Kelley, J.T. 1996: Integratedhigh-precision analyses of Holocene relative sea-level changes:Lessons from the coast of Maine. *Geological Society of America Bulletin 108*, 1073-1088.

Gehrels, W.R., Roe, H.M. & Charman, D.J. 2001: Foraminifera, testate amoebae and diatoms as sea-level indicators in UK saltmarshes: a quantitative multiproxy approach. *Journal of Quaternary Science 16*, 201–220.

Giot, P.-R. 1969: Chronique des datations radiocarbone armoricaines. *Annales de Bretagne 76*, 153-162.

Goldstein, S.T., Watkins, G.T. & Kuhn, R.M. 1995: Microhabitats of salt marsh foraminifera: St. Catherines Island, Georgia, USA. *Marine Micropaleontology 26*, 17-29.

Goldstein, S.T. & Watkins, G.T. 1999: Taphonomy of salt marsh foraminifera: an example from coastal Georgia. *Palaeogeography, Palaeoclimatology, Palaeoecology 149*, 103-114.

Goslin, J., Van Vliet-Lanoë, B., Stephan, P., Delacourt, C., Fernane, A., Gandouin, E., Hénaff, A., Penaud, A. & Suanez, S. 2013: Holocene relative sea level changes in western Brittany (France) between 8000 and 4000 cal.yr B.P: reconstitution from basal-peat deposits. *Géomorphologie: reliefs, processus, environnements 4*, 425-444.

Goslin, J. 2014: *Holocene relative sea-level reconstructiuon in the Finistère region (Brittany, France): regional dynamics, local responses*. Ph.D. thesis, University of Brest, 355 pp.

Goubert, E. 1997: *Les Elphidium excavatum (Terquem), foraminifères benthiques, vivants en baie de Vilaine (Bretagne, France) d'octobre 1992 à septembre 1996: morphologie, dynamique de population en relation avec l'environnement*. Ph.D. thesis, University of Nantes, 186 pp.

Guilcher, A., Bodéré, J.-C. & Hallégouët, B. 1990: Coastal evolution in western, southestern and northern Brittany as a regional test of impact of sea level rise. *Journal of Coastal Research 9*, 67-90.

Guilcher, A. & Hallégouët, B. 1991: Coastal dunes in Brittany and their management. *Journal of Coastal Research 7*, 517-533.

Hallégouët, B. 1971: *Le Bas-Léon. Etude géomorphologique*. Ph.D. thesis, University of Brest, 347 pp.

Hamilton, S. & Shennan, I. 2005: Late Holocene relative sea-level changes and the earthquake deformation cycle around upper Cook Inlet, Alaska. *Quaternary Science Reviews 24*, 1479-1498.

Hayward, B.W., Holzmann, M., Grenfell, H.R., Pawlowski, J. & Triggs, C.M. 2004: Morphological distinction of molecular types in Ammonia - towards a taxonomic revision of the world's most commonly misidentified foraminifera. *Marine Micropaleontology 50*, 237-271.

Hippensteel, S.P., Martin, R.E., Nikitina, D. & Pizzuto, J. 2000: The transformation of Holocene marsh foraminifera assemblages, Middle Atlantic Coast, USA: implications for Holocene sea-level changes. *Journal of Foraminiferal Research 30*, 272-293.

Horton, B.P. & Edwards, R.J. 2003: Seasonal distributions of foraminifera and their implications for sea-level studies, Cowpen Marsh, U.K. *In* Olson, H.C. & Leckie, R.M. (eds.): *Micropaleontologic proxies for sea-level change and stratigraphic discontinuities*, 21-30. *SEPM Special Publication 75*.

Horton, B.P. & Edwards, R.J. 2005: The application of local and regional transfer functions to the reconstruction of Holocene sea levels, north Norfolk, England. *The Holocene 15*, 216-228.

Horton, B.P. & Edwards, R.J. 2006: Quantifying Holocene sea-level change using intertidal foraminifera: lessons from the British Isles. *Cushman Foundation for Foraminiferal Research 40*, 1-97.

Horton, B.P., Edwards, R.J. & Lloyd, J.M. 2000: Implications of a microfossil-based transfer function in Holocene sea-level studies. *In* Shennan, I. & Andrews, J. (eds.): *Holocene land-ocean interaction*

and environmental change around the North Sea, 41-54. *Geological Society, London, Special Publication 166.*

Juggins, S. 2004: C2, Version1.4. WWW Page. Newcastle University, UK. http://www.campus.ncl.ac.uk/staff/Stephen.Juggins/index.html.

Kemp, A.C., Horton, B.P., Vann, D.R., Engelhart, S.E., Grand Pre, C.A., Vane, C.H., Nikitina, D. & Anisfeld, S.C. 2012: Quantitative vertical zonation of salt-marsh foraminifera for reconstructing former sea level; an example from New Jersey, USA. *Quaternary Science Reviews 54*, 26-39.

Lambeck, K. 1997: Sea-level change along the French Atlantic and Channel coast since the time of the Last Glacial Maximum. *Palaeogeography, Palaeoclimatology, Palaeoecology 129*, 1-22.

Leorri, E., Horton, B.P. & Cearreta, A. 2008a: Development of a foraminifera-based transfer function in the Basque marshes, N. Spain : implications for sea-level studies in the Bay of Biscay. *Marine Geology 251*, 60-74.

Leorri, E., Cearreta, A. & Horton, B.P. 2008b: A foraminifera-based transfer function as a tool for sea-level reconstructions in the southern Bay of Biscay. *Geobios 41*, 787-797.

Leorri, E., Gehrels, W.R., Horton, B.P., Fatela, F. & Cearreta, A. 2010: Distribution of foraminifera in salt marshes along the Atlantic coast of SW Europe: Tools to reconstruct past sea-level variations. *Quaternary International 221*, 104-115.

Leorri, E., Fatela, F., Cearreta, A., Moreno, J., Antunes, C. & Drago, T. 2011: Assessing the performance of a foraminifera-based transfer function to estimate sea-level changes in northern Portugal. *Quaternary Research 75*, 278-287.

Leorri, E., Cearreta, A. & Miles, G. 2012: Field observations and modelling of Holocene sea-level changes in the southern Bay of Biscay: implication for understanding current rates of relative sea-level change and vertical land motion along the Atlantic coast of SW Europe. *Quaternary Science Reviews 42*, 59-73.

Lespez, L., Clet-Pellerin, M., Davidson, R., Hermier, G., Carpentier, V. & Cador, J.-M. 2010: Middle to Late Holocene landscape changes and geoarchaeological implications in the marshes of the Dives estuary (NW France). *Quaternary International 216*, 23-40.

Long, A.J. & Hughes, P.D.M. 1995: Mid- and late-Holocene evolution of the Dungeness foreland, UK. *Marine Geology 124*, 253-271.

Long, A.J., Waller, M.P. & Stupples, P. 2006: Driving mechanisms of coastal change: peat compaction and the destruction of late Holocene coastal wetlands. *Marine Geology 225*, 63-84.

Magny, M. 2004: Holocene climate variability as reflected by mid-European lake-level fluctuations and its probable impact on prehistoric human settlements. *Quaternary International 113*, 65-79.

Massey, A.C., Gehrels, W.R., Charman, D.J. & White, S.V. 2006: An intertidal foraminifera-based transfer function for reconstructing Holocene sea-level change in Southwest England. *Journal of Foraminiferal Research 36*, 215-232.

Massey, A.C., Gehrels, W.R., Charman, D.J., Milne, G.A., Peltier, W.R., Lambeck, K. & Selby, K.A. 2008: Relative sea-level change and postglacial isostatic adjustment along the coast of south Devon, United Kingdom. *Journal of Quaternary Science 23*, 415-433.

Morzadec-Kerfourn, M.-T. 1969: Variations de la ligne de rivage au cours du post-glaciaire le long de la côte nord du Finistère. Analyses polliniques de tourbes et de dépôts organiques littoraux. *Bulletin de l'Association Française pour l'Etude du Quaternaire 4*, 285-318.

Morzadec-Kerfourn, M.-T. 1975: Evolution paléogéographique du marais de Dol-de-Bretagne (Ille-et-Vilaine) durant le Flandrien. *Bulletin de la Société Geologique et Minéralogique de Bretagne 7*, 49-51.

Morzadec-Kerfourn, M.T. 1995: Coastline changes in the Armorican Massif (France) during the Holocene. *Journal of Coastal Research 17*, 197-203.

Moulinier, M. 1966: Variabilité d'une population d'Elphidium de la rade de Brest (Nord Finistère) apparentés à Elphidium crispum (Linné). *Revue de Micropaléontologie 9*, 124-200.

Moura, D., Veiga-Pires, L., Albardeiro, T., Boski, T., Rodrigues, A.L. & Tareco, H. 2007: Holocene sea level fluctuations and coastal evolution in the central Algarve (southern Portugal). *Marine Geology 237*, 127-142.

Pailler, Y., Stéphan, P., Gandois, H., Nicolas, C., Sparfel, Y., Tresset, A., Donnart, K., Dréano, Y., Fichaut, B., Suanez, S., Dupont, C., Le Clézio, L., Marcoux, N., Pineau, A., Salanova, L., Sellami, F., Debue, K., Josselin, J. & Dietsch-Sellami, M.-F. 2011: Evolution des paysages et occupation humaine en mer d'Iroise (Finistère, Bretagne) du Néolithique à l'Âge du Bronze. *Norois 220*, 39-68.

Patterson, R.T., Guilbault, J.P. & Clague, J.J., 1999: Taphonomy of tidal foraminifera: implications of surface sample thickness for high-resolution sea-level studies. *Palaeogeography, Palaeoclimatology, Palaeoecology 149*,199-211.

Picado, A., Lopes, C.L., Mendes, R., Vaz, N. & Dias, J.M. 2013: Storm surge impact in the hydrodynamics of a tidal lagoon: the case of Ria de Aviero. *In* Conley, D.C., Masselink, G., Russell,

P.E. & O'Hare, T.J. (eds.): *Proceedings 12th International Coastal Symposium (Plymouth, England)*, 796-801. *Journal of Coastal Research, Special Issue 65*.

Pontee, N.I., Tastet, J.P. & Massé, L. 1998: Morpho-sedimentary evidence of Holocene coastal changes near the mouth of the Gironde and on the Medoc Peninsula, SW France. *Oceanologica Acta 21*, 243-261.

Redois, F. & Debenay, J.-P. 1996: Influence du confinement sur la répartition des foraminifères benthiques: exemple de l'estran d'une ria mésotidale de Bretagne méridionale. *Revue de Paléobiologie 15*, 243-260.

Reimer, P.J., Bard, E., Bayliss, A., Beck, J.W., Blackwell, P.J., Ramsey, C.B., Buck, C.E., Cheng, H., Edwards, R.L., Friedrich, M., Grootes, P.M., Guilderson, T.P., Haflidason, H., Hajdas, I., Hatte, C., Heaton, T.J., Hoffmann, D.L., Hogg, A.G., Hughen, K.A., Kaiser, K.F., Kromer, B., Manning, S.W., Niu, M., Reimer, R.W., Richards, D.A., Scott, E.M., Southon, J.R., Staff, R.A. Turney, C.S.M. & Van Der Plicht, J. 2013: Intcal13 and Marine13 radiocarbon age calibration curves 0-50,000 years cal BP. *Radiocarbon 55*, 1869-1887.

Reineck, H.E. & Singh, I.B. 1980: *Depositional Sedimentary Environments*. 549 pp. Springer Study Edition, Berlin.

Rossi, V., Horton, B.P., Corbett, D.R., Leorri, E., Perez-Belmonte, L. & Douglas, B.C. 2011: The application of foraminifera to reconstruct the rate of 20th century sea level rise, Morbihan Golfe, Brittany, France. *Quaternary Research 75*, 24-35.

Saffert, H. & Thomas, E. 1998: Living foraminifera and total populations in salt marsh peat cores: Kelsey Marsh (Clinton, CT) and the Great Marshes (Barnstable, MA). *Marine Micropalaeontology 33*, 175-202.

Sejrup, H.P., Birks, H.P.B., Kristensen, D.K. & Madsen, H. 2004: Benthonic foraminiferal distributions and quantitative transfer functions for the northwest European continental margin. *Marine Micropalaeontology 53*, 197-226.

Shennan, I. 1986: Flandrian sea-level changes in the Fenland I. The geographical setting and evidence of relative sea-level changes. *Journal of Quaternary Science 1*, 119-54.

Shennan, I. & Horton, B.P. 2002: Holocene land- and sea-level changes in Great Britain. *Journal of Quaternary Science 17*, 511-526.

SHOM. 2013: *Marine Altimetric References, Cotes du zéro hydrographique et niveaux caractéristiques de la marée*. 113 pp. Edition SHOM, Brest.

Sorrel, P., Tessier, B., Demory, F., Delsinne, N. & Mouazé, D. 2009: Evidence for millennialscale climatic events in the sedimentary infilling of a macrotidal estuarine system, the Seine estuary (NW France). *Quaternary Science Reviews 28*, 499-516.

Sorrel, P., Tessier, B., Demory, F., Baltzer, A., Bouaouina, F., Proust, J.-N., Menier, D. & Traini, C. 2010: Sedimentary archives of the French Atlantic coast (inner Bay of Vilaine, south Brittany): Depositional history and late Holocene climatic and environmental signals. *Continental Shelf Research 30*, 1250–1266.

Stéphan, P. 2011a: Colmatage sédimentaire des marais maritimes et variations relatives du niveau marin au cours des 6000 dernières années en rade de Brest (Finistère). *Norois 220*, 9-37.

Stéphan, P. 2011b: *Les flèches de galets de Bretagne: évolution passée, présente et future*. 263 pp. L'Harmattan, Paris.

Stéphan, P. 2011c: Quelques données nouvelles sur la mobilité récente et le bilan sédimentaire des flèches de galets de Bretagne. *Géomorphologie: reliefs, processus, environnements 2*, 205-232.

Stéphan, P., Pailler, Y., Tresset, A. & Gandois, H. 2013: Changements paléogéographiques de l'archipel de Molène (Finistère, Bretagne, France): implications sur les peuplements humains du Néolithique à l'Age du Bronze. *In* Daire, M.-Y., Dupont, C., Baudry, A., Billard, C., Large, J.-M., Lespez, L., Normand, E. & Scarre, C. (eds.): *Ancient maritime communities and the relationship between people and environment along the European Atlantic coasts*, 647-660. Proceedings of the HOMER 2011 Conference, British Archaeological Reports, International Series, Oxford.

Stuiver, M. & Reimer, P.J. 1993: Extended ^{14}C data base and revised CALIB.3.0. ^{14}C age calibration program. *Radiocarbon 35*, 215-230.

Suanez, S., Dehouck A. & Stéphan, P. 2008: Incertitude de la mesure de terrain en géomorphologie littorale. Approche statistique et quantification des marges d'erreur. *In* Allard, P., Fox, D. & Picon, B. (eds.): *Incertitude et environnement, la fin des certitudes scientifiques*, 127-139. Edition EDISUD, Aix-en-Provence.

Swindles, G.T., Lawson, I.T., Matthews, I.P., Blaauwc, M., Daley, T.J., Charman, D.J., P.Rolandf, T., Plunkett, G., Schettler, G., Gearey, B.R., Turner, T.E., Rea, H.A., Roe, H.M., Amesbury, M.J., Chambers, F.M., Holmes, J., Mitchell, F.J.G., Blackford, J., Blundell, A., Branch, N., Holmes, J., Langdon, P., McCarroll, J., McDermott, F., O.Oksanenk, P., Pritchard, O., Stastney, P., Stefanini, B., Young, D., Wheeler, J., Becker, K. & Armit, I. 2013: Centennial-scale climate change in Ireland during the Holocene. *Earth-Science Reviews 126*, 300-320.

Tastet, J.P. & Pontee, N.I. 1998: Morpho-chronology of coastal dunes in Médoc. A new interpretation of Holocene dunes in Southwestern France. *Geomorphology 25*, 93-109.

Ter Braak, C.J.F. & Smilauer, P. 1998: *CANOCO Reference Manual and User's Guide to Canoco for Windows: Software for Canonical Community Ordination (Version 4).* 500 pp. Microcomputer Power, New York.

Ters, M. 1986: Variations in Holocene sea-level on the french Atlantic coast and their climatic significance. *In* Rampino, M.R., Sanders, J.E., Newman, W.S. & Königsson, L.K. (eds.): *Climate: history, periodicity and predictability*, 204-237. Van Nostrand Reinhold, New York.

Tessier, B., Delsinne, N. & Sorrel, P. 2010a: Holocene sedimentary infilling of a tidedominated estuarine mouth. The example of the macrotidal Seine estuary (NW France), *Bulletin de la Société Geologique de France 181*, 87-98.

Tessier, B., Billeaud, I. & Lesueur, P. 2010b: Stratigraphic organization of a composite macrotidal wedge: the Holocene sedimentary infill of the Mont-Saint-Michel Bay. *Bulletin de la Société Geologique de France 181*, 99-113.

Tessier, B., Billeaud, I., Sorrel, P., Delsinne, N. & Lesueur, P. 2012: Infilling stratigraphy of macrotidal tide-dominated estuaries. Controlling mechanisms: Sea-level fluctuations, bedrock morphology, sediment supply and climate changes (The examples of the Seine estuary and the Mont-Saint-Michel Bay, English Channel, NW France). *Sedimentary Geology 279*, 62-73.

Tisdall, E.W., McCulloch, R.D., Sanderson, D.C.W, Simpson, I.A. & Woodward, N.L. 2013: Living with sand: A record of landscape change and storminess during the Bronze and Iron Ages Orkney, Scotland. *Quaternary International 308-309*, 205-215.

Törnqvist, T.E., Van Ree, M.H.M., Van't Veer, R. & Van Geel, B. 1998: Improving methodology for high-resolution reconstruction of sea-level rise and neotectonics by paleoecological analysis and AMS ^{14}C dating of basal peats. *Quaternary Research 49*, 72-85.

Van de Plassche, O. 1986: *Sea-level research: a manual for the collection and evaluation of data*. 618 pp. Geobooks, Norwich.

Van de Plassche, O. 1991: Coastal submergence of the Netherlands, NW Brittany (France), Delmarva Peninsula (VA, USA) and Connecticut (USA) during the last 5500 to 7500 sidereal years. *In* Sabadini, R. (ed.): *Glacial isostasy, sea level and mantle rheology*, 285-300. Kluwer, Dordrecht.

Van de Plassche, O. 1995: Evolution of the intra-coastal tidal range in the Rhine-Meuse delta and Flevo Lagoon, 5700-3000 yrs cal B.C. *Marine Geology 124*, 113-128.

Van Geel, B., Buurman, J., Waterbolk, H.T. 1996: Archaeological and palaeoecological indications of an abrupt climate change in the Netherlands, and evidence for climatological teleconnections around 2650 BP. *Journal of Quaternary Science 11*, 451-460.

Visset, L. & Bernard, J. 2006: Evolution du littoral et du paysage, de la presqu'île de Rhuys à la rivière d'Etel (Massif armoricain - France), du Néolithique au Moyen Âge. *Revue d'archéométrie 30*, 143-156.

Visset, L., Sellier, D. & L'Helgouach, J. 1995: Le paléoenvironnement de la région de Carnac. Sondage dans le marais de Kerdual, La Trinité-sur-Mer (Morbihan). *Revue Archéologique de l'Ouest 12*, 57-71.

Wang, Y., Frank Bohlen, W. & O'Donnell, J. 2000: Storm enhanced bottom shear stress and associated sediment Entrainment in a moderate energetic estuary. *Journal of Oceanography 56*, 311-317.

Watcham, E.P., Shennan, I. & Barlow, N.L.M. 2013: Scale considerations in using diatoms as indicators of sea level change: lessons from Alaska. *Journal of Quaternary Science 28*, 165-179.

Woodroffe, S.A. & Long, A.J. 2009: Salt marshes as archives of recent relative sea level change in West Greenland. *Quaternary Science Reviews 28*, 1750-1761.

Figure captions

Fig. 1. Location maps of studied areas. A. Location of coastal sites used to produce SLIPs from previous sea-level data (see Table 5 for more details) along the coasts of Brittany (France). B. Location of coastal sites studied in this paper (see Fig. 2 for more details).

Fig. 2. Position of drillings and cross-marsh transects. A. Bay of Tresseny. B. Tresseny salt-marshes. C. Porzguen back-barrier salt-marsh (Bay of Brest). D. Lanveur salt-marsh (Bay of Brest). E. Troaon back-barrier salt-marsh (Bay of Brest). F. Arun back-barrier salt-marsh (Bay of Brest). Dots indicate position of gouge augered drillings. Squares indicate position of vibracores used for AMS ^{14}C dating, sedimentological and fossil foraminiferal analyses. White lines correspond to cross-marsh foraminiferal transects along which training sets were collected.

Fig.3. Composition of foraminiferal assemblages from surface sediment samples along cross-marsh transects in the Lanveur and Arun marshes (Bay of Brest) and in the Tresseny salt-marsh.

Fig.4. Observed versus predicted elevation and associated residuals determined by the 'all data' model WAPLS component two (A and B), the 'salt-marsh' model WAPLS component two (C and D), the 'pruned' salt-marsh model WAPLS component three (E and F). The modern samples collected along both Lanveur and Arun cross-marsh transects are distinguished and outliers are highlighted (see text for details).

Fig.5. Observed versus predicted elevation (A) and associated residuals (B) determined by the 'Tresseny model' WAPLS component two.

Fig.6. Detailed stratigraphic cross-section through back-barrier salt-mashes in the Bay of Brest (location of drillings is shown in Fig. 2).

Fig.7. Sedimentology, fossil foraminiferal assemblages and palaeomarsh surface reconstructed elevations. A. Reference Core P-C2 (Porzguen salt-marsh). B. Reference Core T-C2 (Troaon salt-marsh). C. Reference Core A-C10 (Arun salt-marsh). D. Reference Core A-C14 (Arun salt-marsh).

Fig.8. Detailed stratigraphic sections of the inner part of the bay of Tresseny (location is shown in Fig.1).

Fig.9. Sedimentology, fossil foraminiferal assemblages and transfer function reconstructions for Reference Core G-C2 (Bay of Tresseny).

Fig. 10. Mid- to late Holocene RSL plots from the coasts of Brittany. A. SLIPs produced in this study using FBTF reconstructions. SLIPs obtained from samples with 'poor' modern analogues are excluded. Two SLIPs from the basal brackish peat of the Tresseny sediment sequence are also plotted. Numbers correspond to radiocarbon dates presented in Table 2. Black line is the mean trend of RSL rise calculated by a linear regression using the whole SLIPs. B. Plot of SLIPs available in Brittany (see Table 5 for details). The RSL records from North-East, North-West and South-East parts of Brittany are distinguished. Basal SLIPs providing reliable RSL data are highlighted.

Table captions

Table 1. Tide levels relative to French ordonance datum (m NGF) from SHOM 2013.

Table 2. Details of AMS ^{14}C dates obtained from drillings of the West Brittany salt-marshes. Calibrated age based on Intcal13 calibration curve (Reimer *et al*. 2013). Sea-Level index points (SLIPs) obtained from transfer function reconstructions.

Table 3. Transfer function model details. Numbers in bold are cited in the text.

Table 4. Sedimentary facies and associated environments of the Western Brittany salt-marsh sediment infillings.

Table 5. Re-assessment of previous sea-level records from Brittany.

Supporting Information

Table S1. Relative total (dead and alive) abundances of foraminifera taxa found within the modern samples collected from cross-marsh transects at Arun, Lanveur and Tresseny.

Table S2. Relative total (dead and alive) abundances of foraminifera taxa found within the samples collected from the core P-C2 (Porzguen saltmarsh, bay of Brest).

Table S3. Relative total (dead and alive) abundances of foraminifera taxa found within the samples collected from the core T-C2 (Troaon saltmarsh, bay of Brest).

Table S4. Relative total (dead and alive) abundances of foraminifera taxa found within the samples collected from the core A-C14 (Arun saltmarsh, bay of Brest).

Table S5. Relative total (dead and alive) abundances of foraminifera taxa found within the samples collected from the core A-C10 (Arun saltmarsh, bay of Brest).

Table S6. Relative total (dead and alive) abundances of foraminifera taxa found within the samples collected from the core G-C2 (Tresseny saltmarsh).

Study sites	Lowest astronomical tide (LAT)	Mean low water spring tide (MLWST)	Mean low water neap tide (MLWNT)	Mean tide (MT)	Mean high water neap tide (MHWNT)	Mean high water spring tide (MHWST)	Highest astronomical tide (HAT)	Tide gauge location
Bay of Brest, Loc'h beach	-3.38	-2.48	-0.93	0.39	1.86	3.42	4.30	Brest
Bay of Tresseny, Vougot beach, Tariec beach	-3.95	-3.02	-1.27	0.39	2.03	3.68	4.45	Aber Wrac'h
Marais de Dol, Verger Bay	-6.684	-5.124	-2.224	0.426	3.126	6.276	7.746	Cancale
Ploudalmezeau beach	-3.725	-2.855	-1.155	0.465	2.045	3.645	4.505	Portsall
Kerminihy marsh	-1.545	-1.135	-0.485	0.515	1.465	2.265	2.855	Etel
Rohu-Pargo marsh	-2.719	-1.949	-0.699	0.431	1.551	2.651	3.171	Port-Haliguen
Kerdual marsh	-2.754	-2.004	-0.754	0.446	1.496	2.596	3.246	Trinité-sur-Mer
Suscinio marsh	-2.752	-2.012	-0.712	0.518	1.538	2.688	3.338	Pénerf

No	Lab. code	Location	Core	Depth interval in the core (cm)	Elevation (m NGF)	Material	^{14}C a ±1σ	δ ^{13}C	Cal. a BP (2σ) max. (med. prob.) min.	Type of SLIP	MAT diagnostic	RSL (m)	Core sampling	Measure of elevation
1	Erl-10678	Porzguen marsh	P-C2	340-350	-0.05 ; -0.15	Halophytic plant remains	3500±60	-27.2	3615 (3773) 3957	intercalated SLIP	'close' analogues	-3.49	±0.05	±0.13
2	Erl-10679	Porzguen marsh	P-C2	410-420	-0.75 ; -0.85	Halophytic plant remains	4280±60	-27.4	4625 (4852) 5036	intercalated SLIP	'close' analogues	-4.17	±0.05	±0.13
3	Erl-10680	Porzguen marsh	P-C2	470-480	-1.35 ; -1.45	Halophytic plant remains	4640±60	-28.4	5071 (5394) 5581	intercalated SLIP	'close' analogues	-5.32	±0.05	±0.13
4	Erl-10681	Porzguen marsh	P-C2	500-510	-1.65 ; -1.75	Halophytic plant remains	4775±60	-28.6	5324 (5509) 5605	basal SLIP	'poor' analogues	n/a	±0.05	±0.13
5	Erl-10682	Troaon marsh	T-C2	60-70	+2.80 ; +2.70	Halophytic plant remains	940±56	-26.5	734 (850) 952	intercalated SLIP	'close' analogues	-0.48	±0.05	±0.13
6	Erl-10683	Troaon marsh	T-C2	340-350	0.00 ; -0.10	Halophytic plant remains	3690±70	-28.3	3843 (4031) 4235	intercalated SLIP	'close' analogues	-3.35	±0.05	±0.13
7	Erl-10684	Troaon marsh	T-C2	370-380	-0.30 ; -0.40	Halophytic plant remains	4230±60	-28.8	4569 (4744) 4956	intercalated SLIP	'poor' analogues	n/a	±0.05	±0.13
8	Erl-10685	Troaon marsh	T-C2	470-480	-1.30 ; -1.40	Halophytic plant remains	4440±60	-28.7	4872 (5066) 5287	intercalated SLIP	'poor' analogues	n/a	±0.05	±0.13
9	Erl-10686	Troaon marsh	T-C2	500-510	-1.60 ; -1.70	Halophytic plant remains	5450±70	-28.1	6015 (6242) 6399	intercalated SLIP	'close' analogues	-5.32	±0.05	±0.13
10	Erl-11753	Arun marsh	A-C10	90-100	+2.62 ; +2.52	wood fragment	1081± 56	-24.1	916 (999) 1174	intercalated SLIP	'close' analogues	-0.61	±0.05	±0.13
11	Erl-11749	Arun marsh	A-C14	40-50	+3.10 ; +3.00	Halophytic plant remains	436±55	-24.3	316 (483) 546	intercalated SLIP	'close' analogues	-0.30	±0.05	±0.13
12	Erl-11750	Arun marsh	A-C14	140-150	+2.10 ; +2.00	Halophytic plant remains	1686±56	-25.8	1415 (1597) 1720	intercalated SLIP	'close' analogues	-0.97	±0.05	±0.13
13	Erl-11751	Arun marsh	A-C14	270-280	+0.80 ; +0.70	wood fragment	2340±54	-26.6	2159 (2372) 2691	intercalated SLIP	'good' analogues	-2.26	±0.05	±0.13
14	Erl-11752	Arun marsh	A-C14	360-370	-0.10 ; -0.20	wood fragment	2716±55	-27.2	2748 (2822) 2941	basal SLIP	'close' analogues	-2.96	±0.05	±0.13
15	UBA 15681	Tresseny marsh	G-C2	54-56	+3.21 ; +3.19	Halophytic plant remains	431±28	-28.5	338 (500) 527	intercalated SLIP	'good' analogues	-0.28	±0.025	±0.13
16	UBA 15682	Tresseny marsh	G-C2	114-116	+2.61 ; +2.59	Halophytic plant remains	1819±28	-28.4	1825 (1761) 1631	n/a	n/a	n/a	±0.01	±0.13
17	UBA 15683	Tresseny marsh	G-C2	154-156	+2.21 ; +2.19	Halophytic plant remains	2522±32	-27.6	2744 (2597) 2490	n/a	n/a	n/a	±0.01	±0.13
18	UBA 15684	Tresseny marsh	G-C2	200-202	+1.75 ; +1.73	Halophytic plant remains	2732±36	-25.7	2921 (2824) 2758	n/a	n/a	n/a	±0.01	±0.13
19	UBA 17893	Tresseny marsh	G-C2	284-286	+0.91 ; +0.89	Halophytic plant remains	2657±22	-25.8	2836 (2764) 2745	n/a	n/a	n/a	±0.01	±0.13
20	UBA 17894	Tresseny marsh	G-C2	339-341	+0.36 ; +0.34	Halophytic plant remains	2690±27	-26.0	2846 (2788) 2755	n/a	n/a	n/a	±0.01	±0.13
21	UBA 17895	Tresseny marsh	G-C2	369-371	+0.06 ; +0.04	Halophytic plant remains	2689±22	-28.3	2844 (2783) 2755	n/a	n/a	n/a	±0.01	±0.13
22	UBA 15685	Tresseny marsh	G-C2	369-371	+0.06 ; +0.04	Halophytic plant remains	2666±25	-27.1	2844 (2770) 2746	n/a	n/a	n/a	±0.01	±0.13
23	UBA 17896	Tresseny marsh	G-C2	449-451	-0.74 ; -0.72	Halophytic plant remains	4148±34	-28.1	4826 (4692) 4572	n/a	n/a	n/a	±0.01	±0.13
24	UBA 17897	Tresseny marsh	G-C2	494-496	-1.19 ; -1.17	Halophytic plant remains	4795±24	-24.7	5592 (5513) 5474	n/a	n/a	n/a	±0.01	±0.13
25	UBA 15686	Tresseny marsh	G-C2	586-588	-2.11 ; -2.13	Detrital *Phragmites*	5563±31	-28.8	6299 (6351) 6403	Basal	n/a	-4.97	±0.01	±0.13
26	UBA 15459	Tresseny marsh	G-C3	513-515	-0.89 ; -0.91	Detrital *Phragmites*	4054±32	-29.4	4426 (4530) 4785	Basal	n/a	-3.75	±0.01	±0.13

Vertical error (m)		
RMSEP (RMSEP 2σ)	Modern analogue sampling	Total (with 2σ)
±0.20 (0.39)	±0.10	±0.48 (0.67)
±0.20 (0.39)	±0.10	±0.48 (0.67)
±0.20 (0.39)	±0.10	±0.48 (0.67)
±0.20 (0.39)	±0.10	±0.48 (0.67)
±0.20 (0.39)	±0.10	±0.48 (0.67)
±0.20 (0.39)	±0.10	±0.48 (0.67)
±0.20 (0.39)	±0.10	±0.48 (0.67)
±0.20 (0.39)	±0.10	±0.48 (0.67)
±0.20 (0.39)	±0.10	±0.48 (0.67)
±0.20 (0.39)	±0.10	±0.48 (0.67)
±0.20 (0.39)	±0.10	±0.48 (0.67)
±0.20 (0.39)	±0.10	±0.48 (0.67)
±0.20 (0.39)	±0.10	±0.48 (0.67)
±0.20 (0.39)	±0.10	±0.48 (0.67)
±0.14 (0.27)	±0.10	±0.39 (0.55)
n/a	n/a	n/a
n/a	n/a	n/a
n/a	n/a	n/a
n/a	n/a	n/a
n/a	n/a	n/a
n/a	n/a	n/a
n/a	n/a	n/a
n/a	n/a	n/a
n/a	n/a	n/a
n/a	n/a	±1.35
n/a	n/a	±1.35

Model description	Performance index	Components C1	C2	C3	C4	C5
Bay of Tresseny	RMSE (m)	0.19	0.12	0.11	0.10	0.10
Tresseny model- WAPLS (DDCA length: 3.540; DDCA stand.dev: 0.4546)	r^2	0.82	0.93	0.95	0.95	0.95
The whole training set used (14 species. 26 samples)	Max Bias (m)	0.24	0.20	0.12	0.10	0.07
Elevation range:1.61 m	r^2jack	0.78	**0.90**	0.90	0.86	0.83
	Max Biasjack (m)	0.26	0.25	0.19	0.24	0.30
	RMSEPjack (m)	0.21	**0.14**	0.14	0.17	0.19
		C1	C2	C3	C4	C5
Bay of Brest	RMSE (m)	0.51	0.44	0.41	0.40	0.40
1-'all data' model- WAPLS (DDCA length: 2.515; DDCA stand.dev: 0.9889)	r^2	0.73	0.80	0.83	0.84	0.84
The whole training set used (14 species. 51 samples)	Max Bias (m)	1.12	0.70	0.64	0.59	0.61
Elevation range: 3.27 m	r^2jack	0.71	0.76	0.76	0.75	0.76
	Max Biasjack (m)	1.21	0.76	0.70	0.71	0.70
	RMSEPjack (m)	0.53	**0.48**	0.49	0.49	0.49
		C1	C2	C3	C4	C5
Bay of Brest	RMSE (m)	0.43	0.37	0.36	0.35	0.34
2-'salt-marsh' model- WAPLS	r^2	0.54	0.65	0.68	0.70	0.71
Samples from tidal-flat removed. training set of 9 species. 43 samples	Max Bias (m)	0.72	0.62	0.50	0.51	0.48
Elevation range: 2.58 m	r^2jack	0.45	0.46	0.45	0.44	0.45
	Max Biasjack (m)	0.75	0.69	0.58	0.98	1.12
	RMSEPjack (m)	0.47	0.50	0.54	0.60	0.61
		C1	C2	C3	C4	C5
Bay of Brest						
3 - 'pruned' salt-marsh model- WAPLS (DDCA length: 2.551; DDCA stand.dev: 0.9154)	RMSE (m)	0.37	0.21	0.17	0.16	0.16
Samples from tidal-flat. tidal-creeks and salt-pans removed.	r^2	0.68	0.90	**0.94**	0.94	0.94
Training set of 8 species. 29 samples	Max Bias (m)	0.63	0.40	0.27	0.29	0.31
Elevation range: 2.35 m	r^2jack	0.56	0.86	0.91	0.90	0.87
	Max Biasjack (m)	0.94	0.48	0.30	0.33	0.39
	RMSEPjack (m)	0.44	0.25	**0.20**	0.22	0.26

Lithofacies	Description	Mean grain size
LF1	Reed peat with phragmites remains	30-60 µm
LF2	Silty clay with salt-marsh plant fragments and rootlets	20-60 µm
LF3	Silty-sand with shell fragments	100 µm
LF4	Grey silty-clay mm-laminated with black organic-rich silt	50-60 µm
LF5	Coarse sand and gravels	800-1200 µm
LF6	Reed peat with phragmites remains and a significant proportion of sand	150-250 µm
LF7	Coarse sand	800-1000 µm
LF8	Minerogenic sandy-silt	100 µm
LF9	Sandy-silt with rootlets and plants debris	50-250 µm

Foraminiferal content	Depositional environment
Occasional presence of high salt-marsh agglutinated foraminifera dominant	Brackish marsh to swamp
High salt-marsh agglutinated foraminifera	High salt-marsh
Salt-marsh agglutinated and calcareous foraminifera	High salt-marsh with mudflat sediment input by storm waves
High salt-marsh agglutinated foraminifera, occasional absence of foraminifera	Back-barrier brackish marsh to freshwater swamp
No foraminifera	Gravel barrier washover fan
Very low foraminiferal density	Dune back-barrier brackish marsh to swamp with eolian sandy input
No foraminifera	Sand-flat or breach in the barrier dune
Very low foraminiferal density	Sand-flat
High salt-marsh agglutinated foraminifera	High salt-marsh

No	Lab. code	Coastal site	Elevation (m NGF)	Material
1	GrN-14138	Marais de Dol	-2.41 ; -2.45	reed peat
2	GrN-14139	Marais de Dol	+0.90 ; +0.94	reed peat
3	GrN-14140	Marais de Dol	+1.48 ; +1.51	reed peat + peaty jyttja
4	GrN-14141	Marais de Dol	+2.03 ; +2.05	amorphous peat
5	GrN-14142	Marais de Dol	+0.65 ; +0.69	reed peat
6	GrN-14143	Marais de Dol	+0.87 ; +0.91	reed peat
7	GrN-14144	Marais de Dol	+1.14 ; +1.17	reed peat
8	GrN-14145	Marais de Dol	-2.71 ; -2.77	peaty jyttja + reed remains
9	GrN-14146	Marais de Dol	+1.53 ; +1.56	oxidized reed peat
10	GrN-14147	Marais de Dol	+1.83 ; +1.87	reed peat + leaf remains
11	GrN-14148	Marais de Dol	+6.23 ; +6.28	reed peat
12	GrN-14149	Marais de Dol	+0.52 ; +0.56	peaty clay + reed remains
13	GrN-14150	Marais de Dol	+1.80 ; +1.83	reed peat
14	GrN-14151	Marais de Dol	+3.05 ; +3.08	reed peat
15	GrN-14152	Marais de Dol	+3.14 ; +3.17	humic clay + vegetation remains
16	GrN-14153	Marais de Dol	+3.32 ; +3.35	oxidized reedpeat + wood remains
17	GrN-14154	Marais de Dol	+1.90 ; +1.94	oxidized reedpeat
18	GrN-14155	Marais de Dol	+2.15 ; +2.17	oxidized peat
19	GrN-14156	Marais de Dol	+1.75 ; +1.79	oxidized peat
20	GrN-14157	Marais de Dol	+2.12 ; +2.15	oxidized peat
21	GrN-14158	Marais de Dol	-0.26 ; -0.30	reed peat
22	GrN-14159	Marais de Dol	+1.48 ; +1.51	peaty clay
23	GrN-14160	Marais de Dol	+2.05 ; +2.09	reed peat
24	GrN-14161	Marais de Dol	+2.30 ; +2.34	reed peat
25	*	Verger bay	-8.10 ; -9.10	Silty-clay + halophitic plant remains
26	*	Verger bay	+2.50 ; +1.50	Silty-clay + halophitic plant remains
27	*	Verger bay	+2.50 ; +1.50	Organic-rich mud
28	UBA-15461	Vougot beach	-1.14 ; -1.16	Detrital *Phragmites*
29	UBA-15460	Vougot beach	-3.51 ; -3.53	Detrital *Phragmites*
30	UBA-15458	Tariec beach	-3.79 ; -3.81	Detrital *Phragmites*
31	Gif-766	Ploudalmezeau beach	-4.40	reed peat
32	Ly-8871	Loc'h beach	+1.64	Wood fragment within organic mud
33	Ly-8870	Loc'h beach	+2.15	Wood fragment within organic mud
34	A10101	Kerminihy marsh	+0.79	reed peat
35	Ly-11481	Rohu-Pargo marsh	+2.43	Silty-clay + halophitic plant remains
36	Beta-185617	Rohu-Pargo marsh	+1.15	Silty-clay + halophitic plant remains
37	Ly-11482	Rohu-Pargo marsh	+0.53	Silty-clay + halophitic plant remains
38	Ly6001	Kerdual marsh	+0.82	Silty-clay + halophitic plant remains
39	Ly6002	Kerdual marsh	+0.27	Silty-clay + halophitic plant remains
40	A9830	Suscinio marsh	-1.57	Silty-clay + halophitic plant remains
41	A9832	Suscinio marsh	-2.77	Silty-clay + halophitic plant remains
42	A9829	Suscinio marsh	-3.37	Silty-clay + halophitic plant remains
43	A9831	Suscinio marsh	-4.15	Silty-clay + halophitic plant remains
44	A9833	Suscinio marsh	-4.87	Silty-clay + halophitic plant remains

Indicative meaning	Indicative range (m)	^{14}C a ±1σ	Cal. a BP (2σ) max. (med. prob.) min.	RSL (m)	Error range (m)	type of SLIP
from MHWNT to HAT	±2.31	6625±35	7572 (7515) 7439	-10.18	±2.8	intercalated SLIP
from MHWNT to HAT	±2.31	5980±60	6955 (6820) 6669	-6.83	±2.8	intercalated SLIP
from MHWNT to HAT	±2.31	5800±45	6726 (6600) 6491	-6.25	±2.8	intercalated SLIP
from MHWNT to HAT	±2.31	5450±35	6302 (6247) 6193	-5.71	±2.8	intercalated SLIP
from MHWNT to HAT	±2.31	6075±45	7155 (6937) 6792	-7.08	±2.8	intercalated SLIP
from MHWNT to HAT	±2.31	5820±40	6730 (6628) 6503	-6.86	±2.8	intercalated SLIP
from MHWNT to HAT	±2.31	5425±40	6302 (6237) 6034	-6.6	±2.8	intercalated SLIP
from MHWNT to HAT	±2.31	6540±70	7569 (7454) 7320	-10.49	±2.8	intercalated SLIP
from MHWNT to HAT	±2.31	5295±35	6185 (6081) 5948	-6.2	±2.8	intercalated SLIP
from MHWNT to HAT	±2.31	4835±35	5645 (5585) 5476	-5.9	±2.8	intercalated SLIP
from MHWNT to HAT	±2.31	2820±30	3016 (2922) 2847	-1.5	±2.8	intercalated SLIP
from MHWNT to HAT	±2.31	6070±45	7155 (6929) 6789	-7.21	±2.8	intercalated SLIP
from MHWNT to HAT	±2.31	5365±35	6277 (6167) 6004	-5.93	±2.8	intercalated SLIP
from MHWNT to HAT	±2.31	4730±60	5587 (5469) 5321	-4.68	±2.8	intercalated SLIP
from MHWNT to HAT	±2.31	4385±40	5213 (4948) 4851	-4.6	±2.8	intercalated SLIP
from MHWNT to HAT	±2.31	4340±35	5030 (4910) 4842	-4.41	±2.8	intercalated SLIP
from MHWNT to HAT	±2.31	5535±30	6398 (6334) 6288	-5.83	±2.8	intercalated SLIP
from MHWNT to HAT	±2.31	5030±35	5895 (5807) 5662	-5.59	±2.8	intercalated SLIP
from MHWNT to HAT	±2.31	4870±35	5661 (5610) 5486	-5.98	±2.8	intercalated SLIP
from MHWNT to HAT	±2.31	4430±35	5277 (5021) 4873	-5.62	±2.8	intercalated SLIP
from MHWNT to HAT	±2.31	5725±40	6635 (6521) 6414	-8.03	±2.8	intercalated SLIP
from MHWNT to HAT	±2.31	5760±60	6712 (6560) 6409	-6.26	±2.8	intercalated SLIP
from MHWNT to HAT	±2.31	5305±35	6190 (6085) 5951	-5.68	±2.8	intercalated SLIP
from MHWNT to HAT	±2.31	4960±35	5842 (5686) 5603	-5.43	±2.8	intercalated SLIP
from MHWNT to HAT	±2.31	7310±80	7977 (8120) 8314	-13.74	±2.8	Basal SLIP
from MHWNT to HAT	±2.31	2630±130	2353 (2727) 3005	-1.36	±2.8	Basal SLIP
from MHWNT to HAT	±2.31	4020±130	4152 (4508) 4839	-3.136	±2.8	Basal SLIP
from MHWNT to HAT	±1.21	4309±38	4970 (4900) 4830	-4.39	±1.3	Basal SLIP
from MHWNT to HAT	±1.21	6033±29	6950 (6870) 6790	-6.74	±1.3	Basal SLIP
from MHWNT to HAT	±1.21	6001±28	6910 (6850) 6780	-6.78	±1.3	Basal SLIP
from MHWNT to HAT	±1.23	5770±150	6933 (6610) 6288	-7.26	±1.7	intercalated SLIP
from MHWNT to HAT	±1.22	1075±40	927 (985) 1061	-1.437	±1.3	intercalated SLIP
from MHWNT to HAT	±1.22	950±25	796 (853) 925	-0.926	±1.3	intercalated SLIP
from MHWNT to HAT	±0.695	2535±65	2379 (2596) 2757	-1.37	±0.8	intercalated SLIP
from MHWNT to HAT	±0.81	1190±50	981 (1118) 1258	0.069	±2	intercalated SLIP
from MHWNT to HAT	±0.81	2810±40	2792 (2913) 3031	-1.211	±1	intercalated SLIP
from MHWNT to HAT	±0.81	3570±35	3726 (3871) 3975	-1.831	±0	intercalated SLIP
from MHWNT to HAT	±0.875	2905±55	2880 (3045) 3207	-1.551	±1	intercalated SLIP
from MHWNT to HAT	±0.875	3155±85	3161 (3370) 3573	-2.101	±1	intercalated SLIP
from MHWNT to HAT	±0.9	4895±70	5471 (5638) 5881	-4.008	±1	intercalated SLIP
from MHWNT to HAT	±0.9	5590±90	6211 (6384) 6626	-5.208	±1	intercalated SLIP
from MHWNT to HAT	±0.9	5700±115	6287 (6502) 6742	-5.808	±1	intercalated SLIP
from MHWNT to HAT	±0.9	5700±80	6316 (6496) 6660	-6.588	±1	intercalated SLIP
from MHWNT to HAT	±0.9	6600±85	7325 (7497) 7617	-7.308	±1	Basal SLIP

Reference
Van de Plassche (1991)
Van de Plassche (1991)
Van de Plassche (1991)
Van de Plassche (1991)
Van de Plassche (1991)
Van de Plassche (1991)
Van de Plassche (1991)
Van de Plassche (1991)
Van de Plassche (1991)
Van de Plassche (1991)
Van de Plassche (1991)
Van de Plassche (1991)
Van de Plassche (1991)
Van de Plassche (1991)
Van de Plassche (1991)
Van de Plassche (1991)
Van de Plassche (1991)
Van de Plassche (1991)
Van de Plassche (1991)
Van de Plassche (1991)
Van de Plassche (1991)
Van de Plassche (1991)
Van de Plassche (1991)
Van de Plassche (1991)
Van de Plassche (1991)
Van de Plassche (1991)
Regnauld *et al.* (1996)
Regnauld *et al.* (1996)
Regnauld *et al.* (1996)
Goslin *et al* . (2013)
Goslin *et al* . (2013)
Goslin *et al* . (2013)
Morzadec-Kerfourn (1969)
Stéphan & Laforge (2013)
Stéphan & Laforge (2013)
Visset & Bernard (2006)
Gaudin (2004)
Gaudin (2004)
Gaudin (2004)
Visset *et al.* (1995)
Visset *et al.* (1995)
Visset & Bernard (2006)
Visset & Bernard (2006)
Visset & Bernard (2006)
Visset & Bernard (2006)
Visset & Bernard (2006)

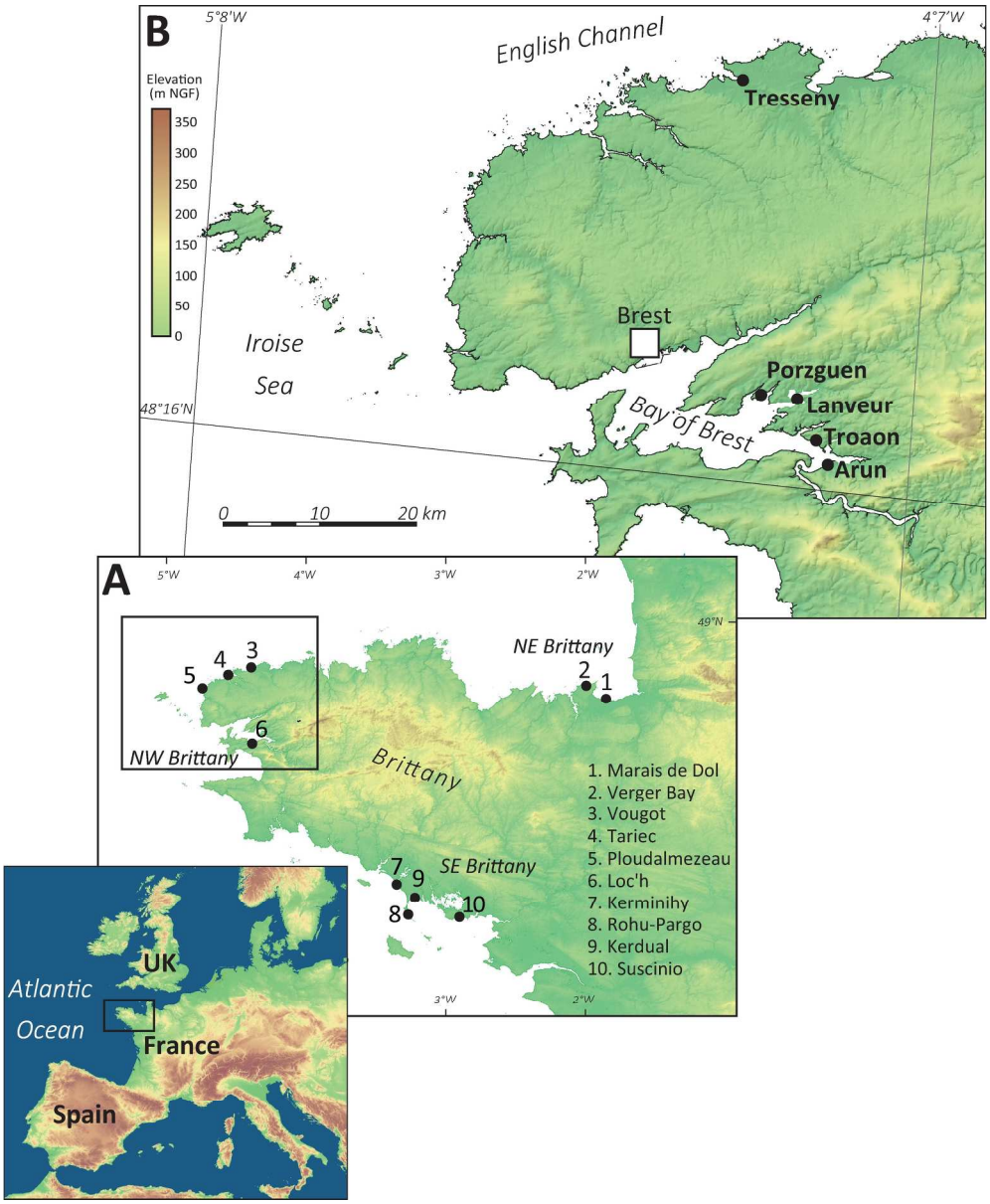

210x255mm (300 x 300 DPI)

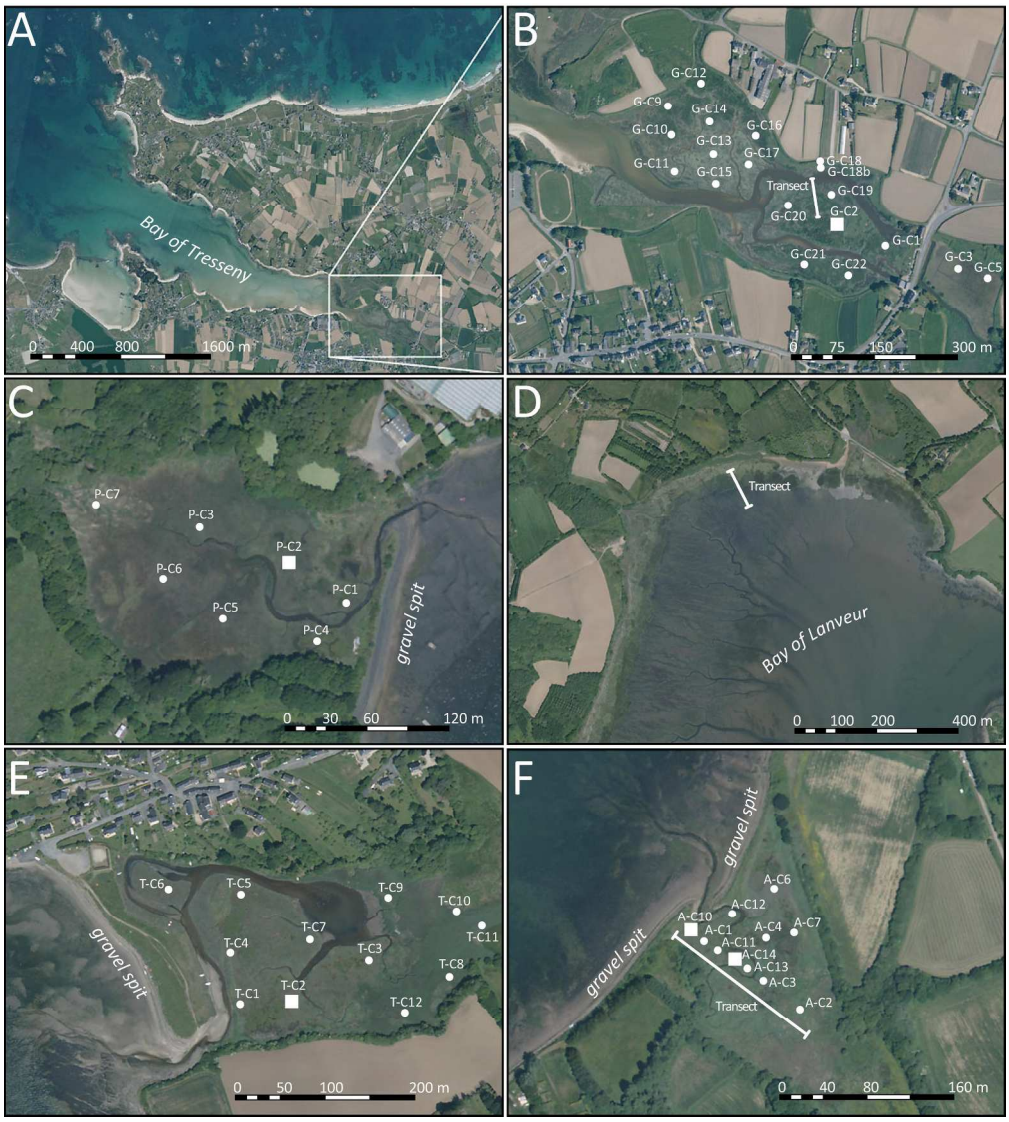

219x244mm (300 x 300 DPI)

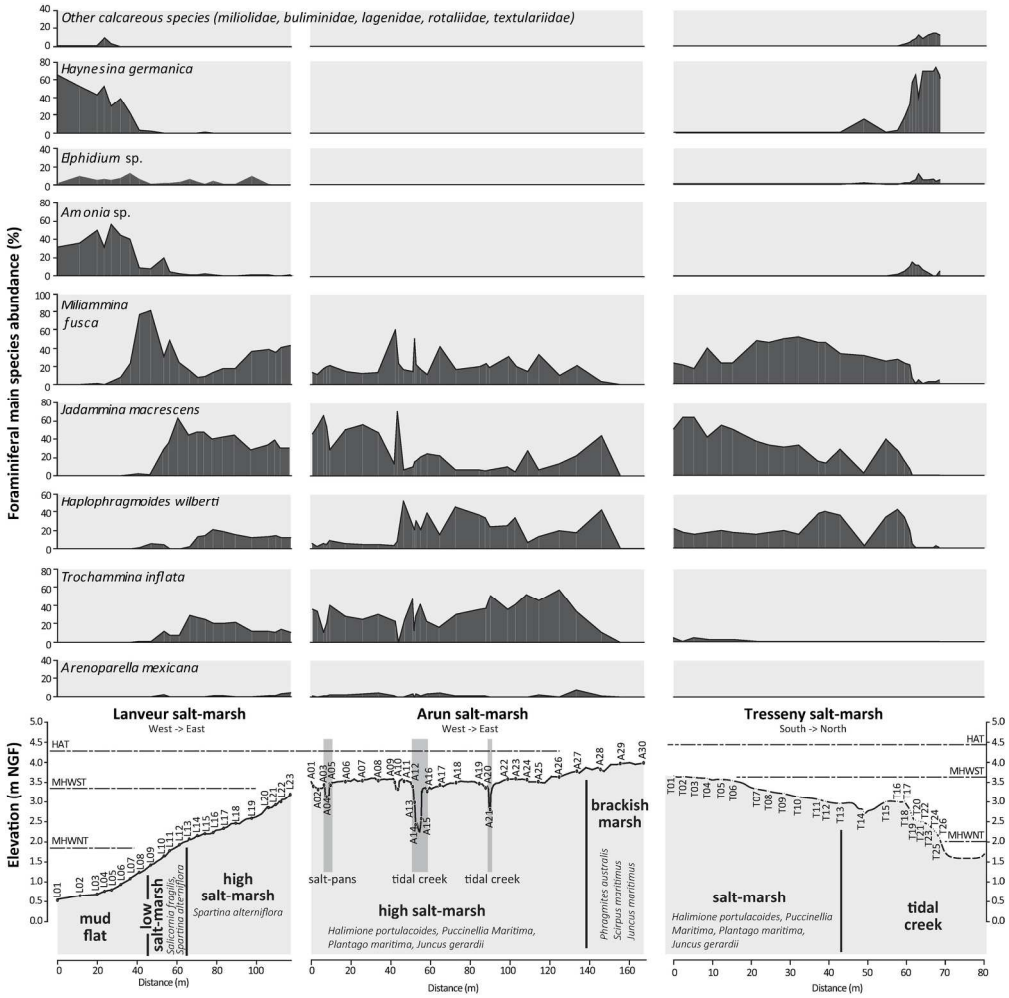

187x185mm (300 x 300 DPI)

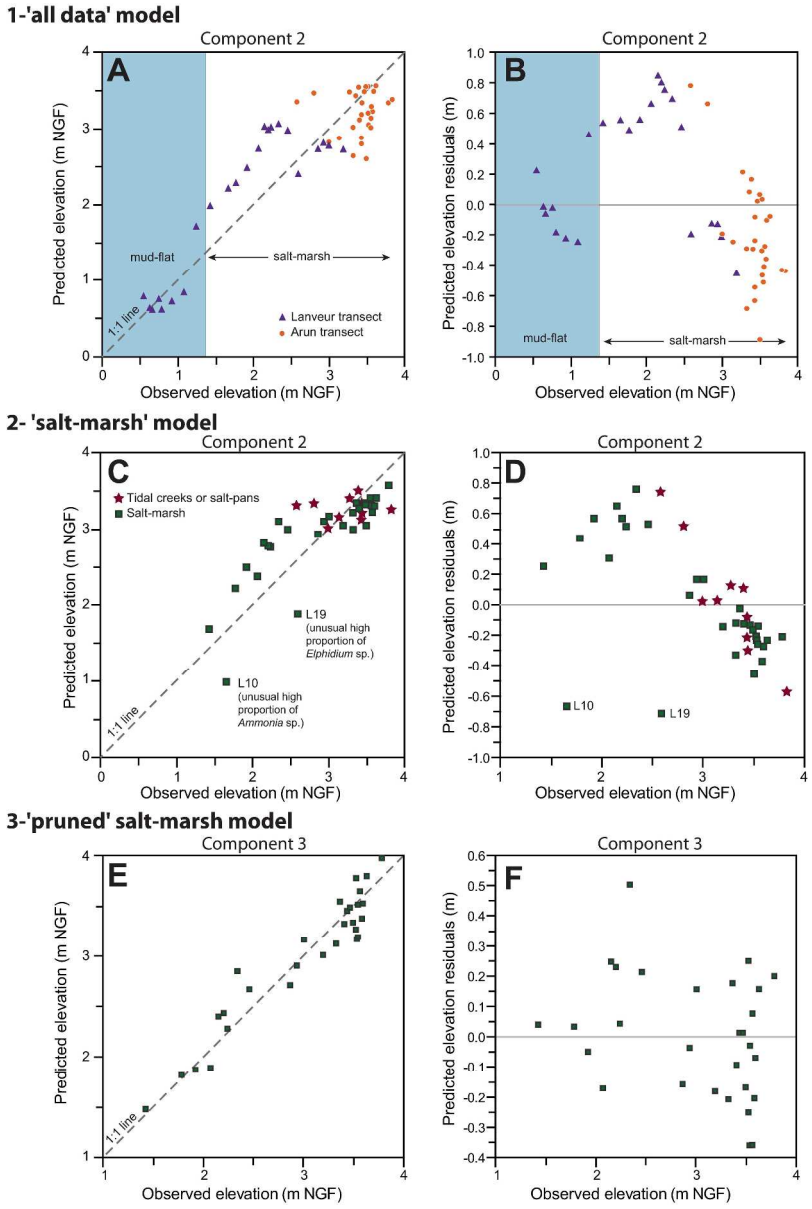

277x414mm (300 x 300 DPI)

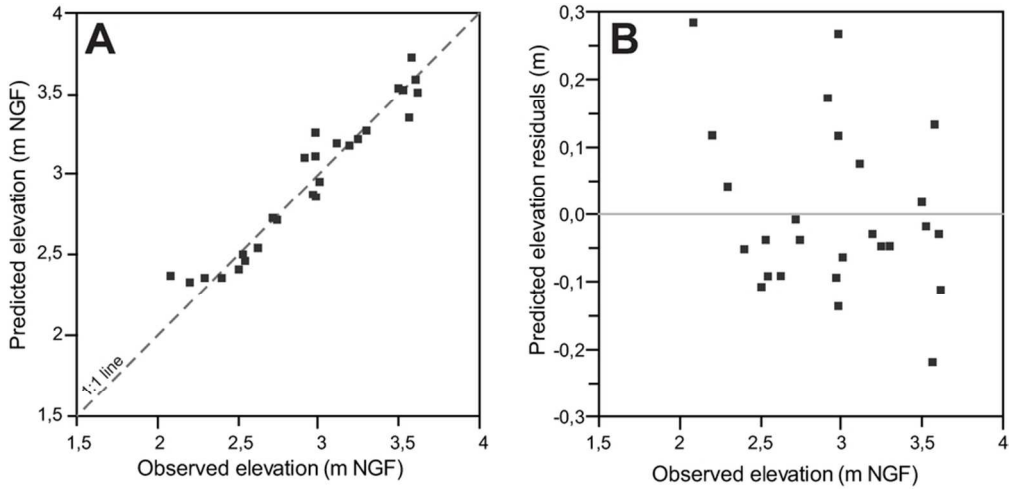

84x40mm (300 x 300 DPI)

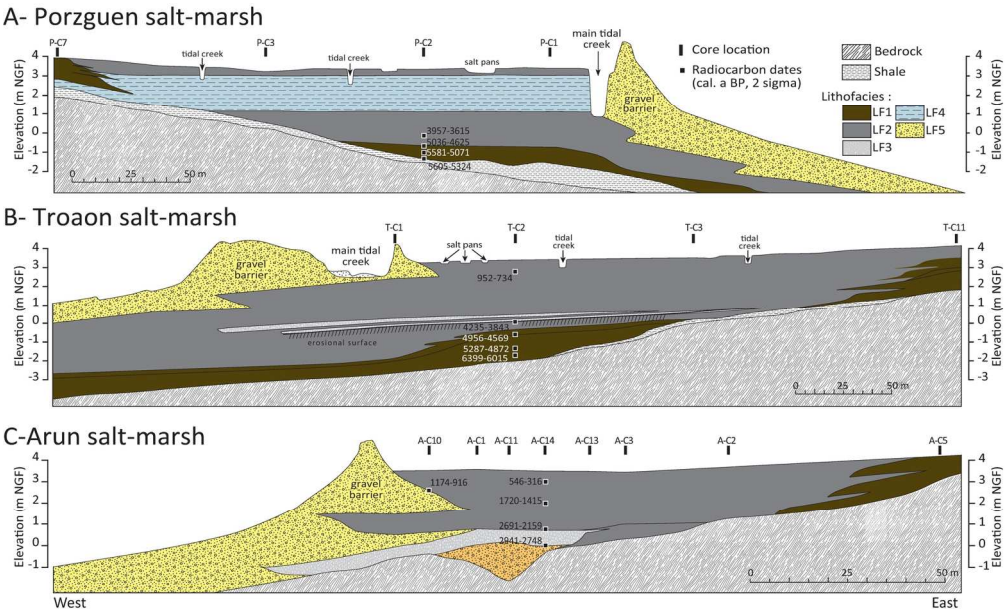

162x98mm (300 x 300 DPI)

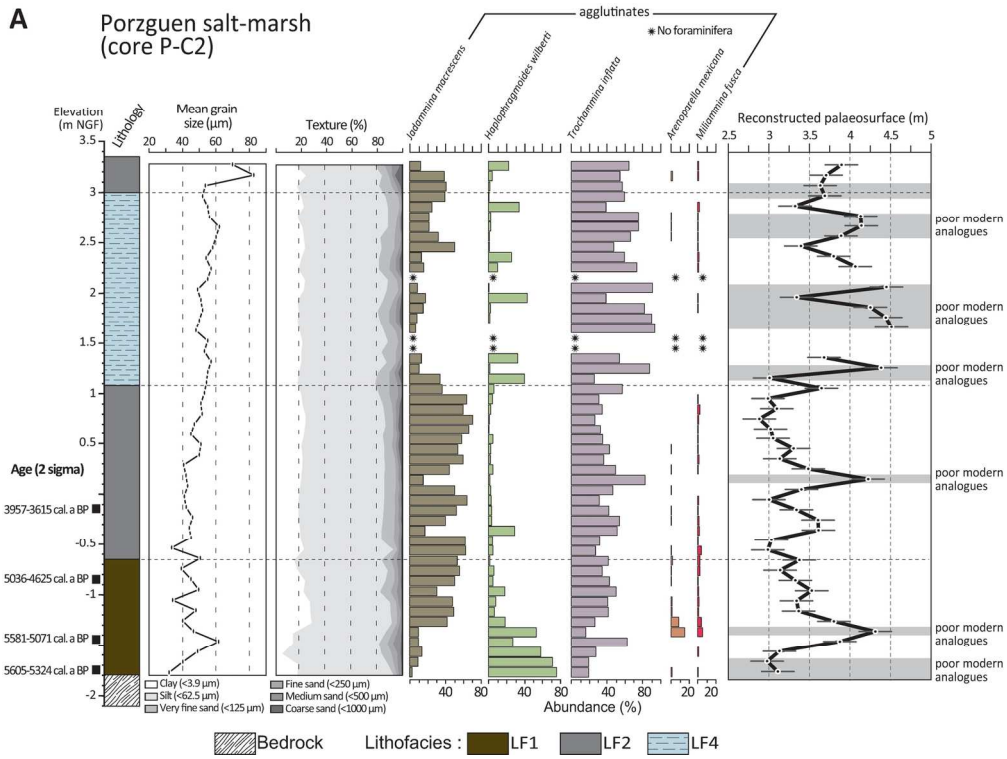

161x121mm (300 x 300 DPI)

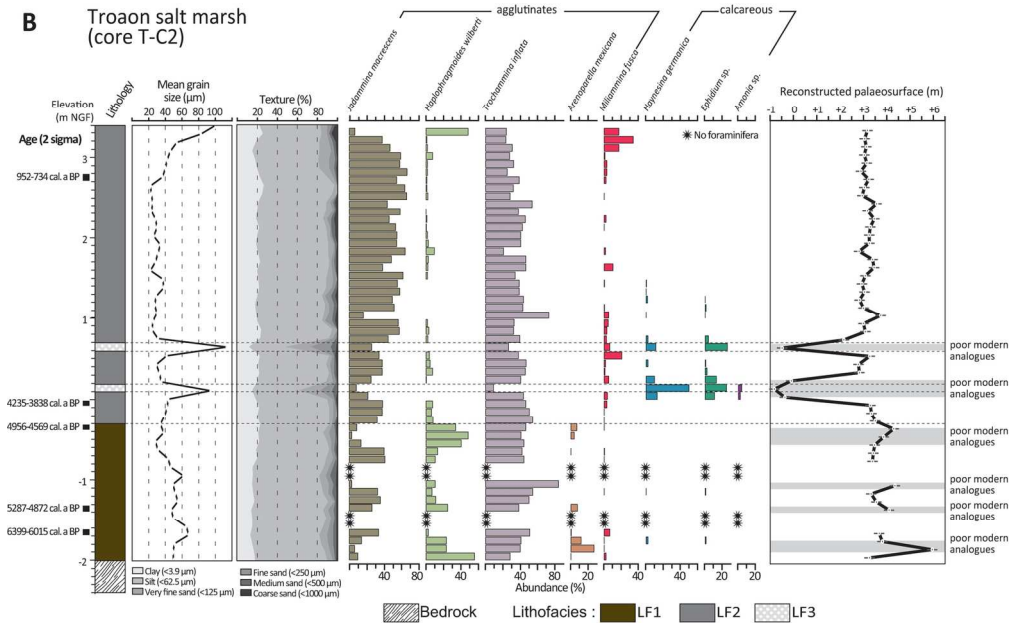

155x96mm (300 x 300 DPI)

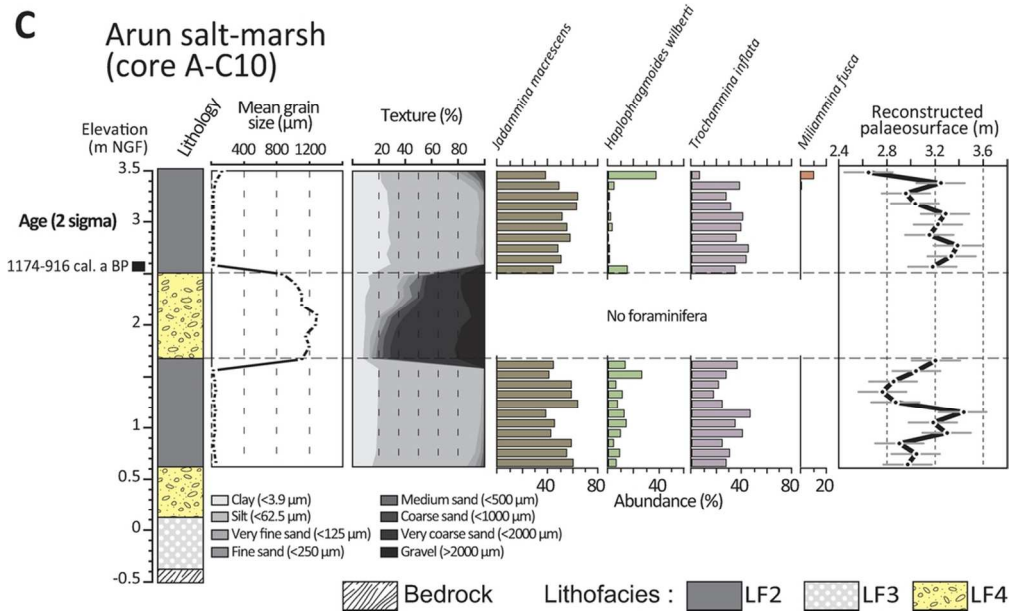

97x59mm (300 x 300 DPI)

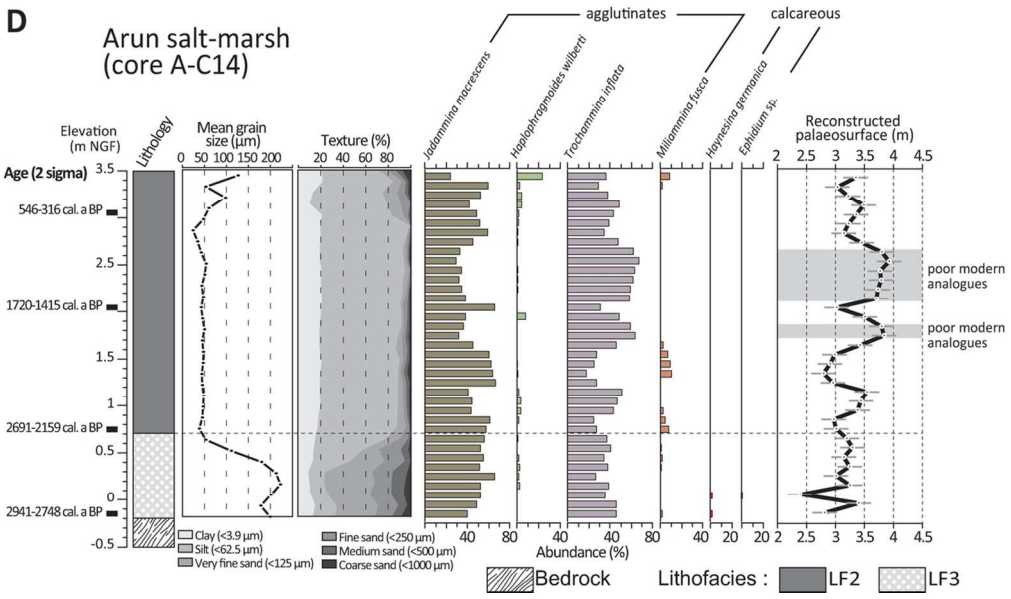

111x65mm (300 x 300 DPI)

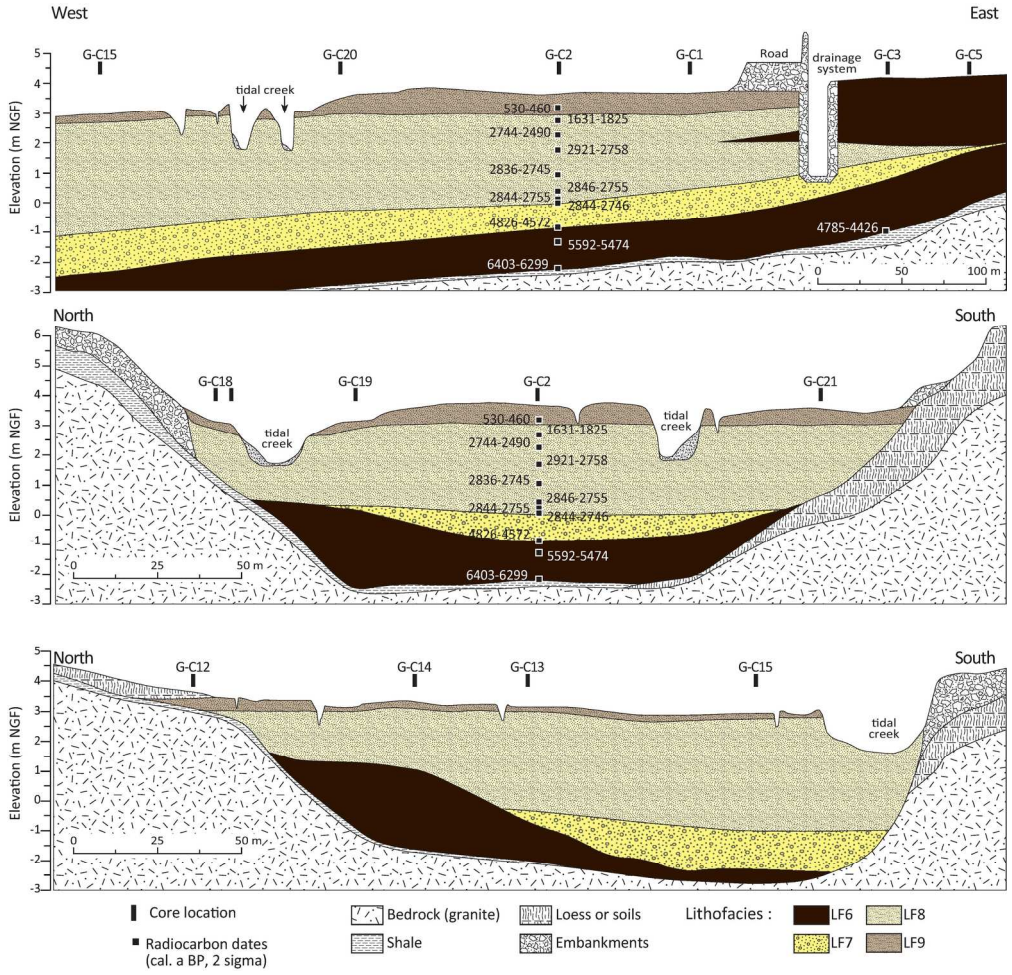

179x173mm (300 x 300 DPI)

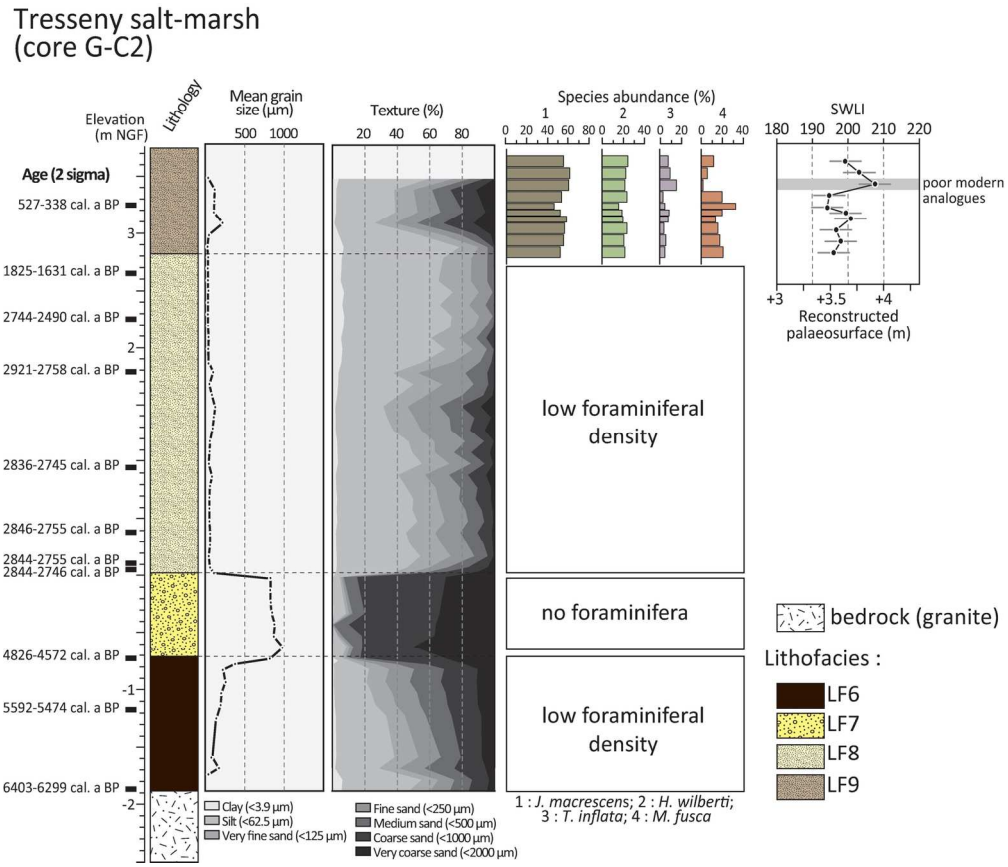

154x132mm (300 x 300 DPI)

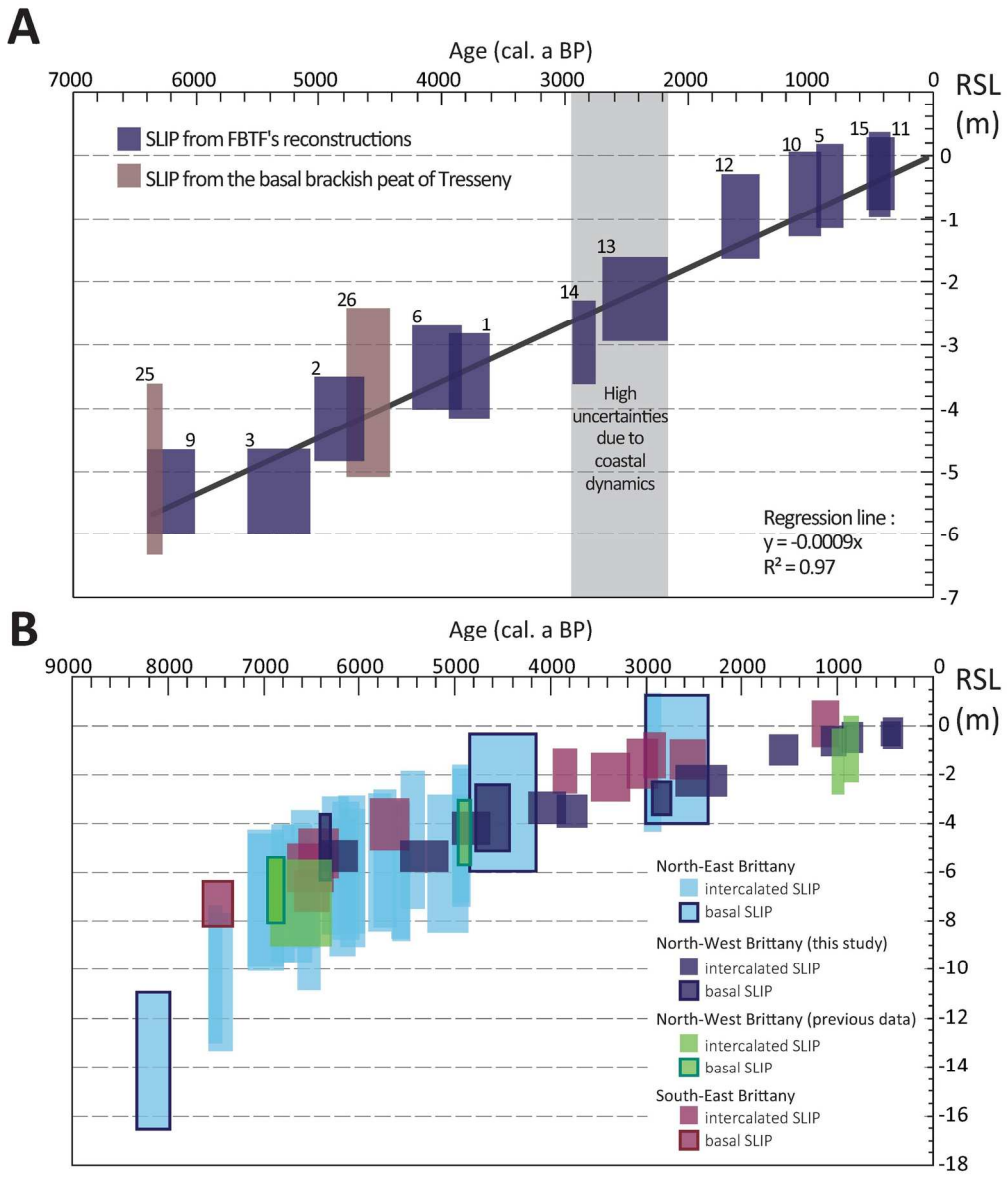

164x194mm (300 x 300 DPI)

Table S1. Relative total (dead and alive) abundances of foraminifera taxa found within the modern samples collected from cross-marsh transects at Arun, Lanveur and Tresseny.

Salt-marsh	Sample code	Elevation (m NGF)	Elevation (SWLI)	*Jadammina macrescens*	*Haplophragmoides wilberti*	*Trochammina inflata*	*Arenoparella mexicana*	*Miliammina fusca*	*Haynesina germanica*	*Elphidium sp.*	*Ammonia sp.*	Other species (A)	(A) Other species: *Lagena sulcata*	*Fissurina lucida*	*Quinqueloculina sp.*	*Favulina squamosa*	*Hopkinsina atlanticus*	*Bolivina variabilis*
Arun	A01	3,40	191,23	46,00	5,00	35,00	1,33	12,67	0,00	0,00	0,00	0,00	0,00	0,00	0,00	0,00	0,00	0,00
Arun	A02	3,32	188,76	53,80	1,98	33,00	0,00	11,22	0,00	0,00	0,00	0,00	0,00	0,00	0,00	0,00	0,00	0,00
Arun	A03	3,44	192,17	65,02	4,95	10,53	1,55	17,96	0,00	0,00	0,00	0,00	0,00	0,00	0,00	0,00	0,00	0,00
Arun	A04	3,13	183,05	53,59	4,58	20,92	0,98	19,93	0,00	0,00	0,00	0,00	0,00	0,00	0,00	0,00	0,00	0,00
Arun	A05	3,43	192,02	28,39	8,71	39,68	2,58	20,65	0,00	0,00	0,00	0,00	0,00	0,00	0,00	0,00	0,00	0,00
Arun	A06	3,52	194,71	50,50	4,95	27,72	2,64	14,19	0,00	0,00	0,00	0,00	0,00	0,00	0,00	0,00	0,00	0,00
Arun	A07	3,55	195,49	55,72	4,82	24,70	2,71	12,05	0,00	0,00	0,00	0,00	0,00	0,00	0,00	0,00	0,00	0,00
Arun	A08	3,55	195,49	47,18	4,87	30,51	4,62	12,82	0,00	0,00	0,00	0,00	0,00	0,00	0,00	0,00	0,00	0,00
Arun	A09	3,50	194,13	12,80	3,05	22,26	1,22	60,67	0,00	0,00	0,00	0,00	0,00	0,00	0,00	0,00	0,00	0,00
Arun	A10	3,33	188,97	69,23	7,69	0,00	0,00	23,08	0,00	0,00	0,00	0,00	0,00	0,00	0,00	0,00	0,00	0,00
Arun	A11	3,53	195,01	6,19	52,12	24,43	0,33	16,94	0,00	0,00	0,00	0,00	0,00	0,00	0,00	0,00	0,00	0,00
Arun	A12	3,43	161,81	16,04	30,72	28,33	2,73	22,18	0,00	0,00	0,00	0,00	0,00	0,00	0,00	0,00	0,00	0,00
Arun	A13	3,39	190,93	10,13	25,49	46,41	3,59	14,38	0,00	0,00	0,00	0,00	0,00	0,00	0,00	0,00	0,00	0,00
Arun	A14	2,99	178,79	15,03	20,81	13,29	0,00	50,87	0,00	0,00	0,00	0,00	0,00	0,00	0,00	0,00	0,00	0,00
Arun	A15	2,58	166,31	20,39	21,04	41,10	0,97	16,50	0,00	0,00	0,00	0,00	0,00	0,00	0,00	0,00	0,00	0,00
Arun	A16	3,28	187,37	24,06	39,52	22,34	3,44	10,65	0,00	0,00	0,00	0,00	0,00	0,00	0,00	0,00	0,00	0,00
Arun	A17	3,44	192,23	22,26	15,48	16,13	3,87	42,26	0,00	0,00	0,00	0,00	0,00	0,00	0,00	0,00	0,00	0,00
Arun	A18	3,50	194,04	6,25	46,13	29,76	0,89	16,96	0,00	0,00	0,00	0,00	0,00	0,00	0,00	0,00	0,00	0,00
Arun	A19	3,47	193,14	6,35	36,51	35,98	1,06	20,11	0,00	0,00	0,00	0,00	0,00	0,00	0,00	0,00	0,00	0,00
Arun	A20	3,36	189,96	5,56	33,33	36,81	1,39	22,92	0,00	0,00	0,00	0,00	0,00	0,00	0,00	0,00	0,00	0,00
Arun	A21	2,81	173,23	6,29	24,25	50,30	0,00	19,16	0,00	0,00	0,00	0,00	0,00	0,00	0,00	0,00	0,00	0,00
Arun	A22	3,58	196,61	9,69	24,69	35,00	0,00	30,63	0,00	0,00	0,00	0,00	0,00	0,00	0,00	0,00	0,00	0,00
Arun	A23	3,59	196,97	4,83	33,51	41,29	0,27	20,11	0,00	0,00	0,00	0,00	0,00	0,00	0,00	0,00	0,00	0,00
Arun	A24	3,57	196,10	26,97	6,25	51,64	0,33	14,80	0,00	0,00	0,00	0,00	0,00	0,00	0,00	0,00	0,00	0,00
Arun	A25	3,52	194,77	6,87	13,49	45,29	1,78	32,57	0,00	0,00	0,00	0,00	0,00	0,00	0,00	0,00	0,00	0,00
Arun	A26	3,63	198,15	13,01	19,86	56,51	0,34	10,27	0,00	0,00	0,00	0,00	0,00	0,00	0,00	0,00	0,00	0,00
Arun	A27	3,78	202,71	21,33	17,00	33,67	7,67	20,33	0,00	0,00	0,00	0,00	0,00	0,00	0,00	0,00	0,00	0,00
Arun	A28	3,82	203,92	42,97	42,19	10,94	0,78	3,13	0,00	0,00	0,00	0,00	0,00	0,00	0,00	0,00	0,00	0,00
Lanveur	L01	0,55	105,14	0,00	0,00	0,00	0,00	0,00	65,15	2,28	31,92	0,65	0,00	0,00	0,65	0,00	0,00	0,00
Lanveur	L02	0,65	108,04	0,00	0,00	0,00	0,00	0,00	53,01	10,24	35,54	1,20	0,00	0,00	1,20	0,00	0,00	0,00
Lanveur	L03	0,68	109,00	0,00	0,00	0,00	0,00	0,66	43,19	5,65	49,83	0,66	0,00	0,00	0,66	0,00	0,00	0,00
Lanveur	L04	0,77	111,54	0,00	0,00	0,00	0,00	0,00	52,98	6,62	31,13	9,27	2,23	1,48	3,71	1,11	0,37	0,37
Lanveur	L05	0,80	112,63	0,00	0,00	0,00	0,00	3,66	30,18	5,79	56,71	3,66	0,73	0,37	2,20	0,37	0,00	0,00
Lanveur	L06	0,95	116,98	0,33	0,33	0,33	0,00	8,17	38,24	7,84	44,77	0,00	0,00	0,00	0,00	0,00	0,00	0,00
Lanveur	L07	1,09	121,42	1,30	0,33	0,33	0,00	22,80	22,48	12,70	40,07	0,00	0,00	0,00	0,00	0,00	0,00	0,00
Lanveur	L08	1,24	125,92	1,69	0,68	1,02	0,00	76,95	3,73	6,44	9,15	0,34	0,00	0,00	0,34	0,00	0,00	0,00
Lanveur	L09	1,43	131,66	1,53	5,34	1,15	0,00	80,92	1,91	1,15	8,02	0,00	0,00	0,00	0,00	0,00	0,00	0,00
Lanveur	L10	1,65	138,37	29,61	4,29	12,02	1,72	30,47	0,43	1,72	19,31	0,43	0,00	0,00	0,43	0,00	0,00	0,00
Lanveur	L11	1,78	142,20	35,50	0,38	8,02	0,00	48,86	0,38	2,29	4,58	0,00	0,00	0,00	0,00	0,00	0,00	0,00
Lanveur	L12	1,93	146,55	62,72	0,00	7,89	0,36	23,66	0,36	2,87	2,15	0,00	0,00	0,00	0,00	0,00	0,00	0,00
Lanveur	L13	2,07	150,90	44,98	2,27	29,45	0,32	14,89	0,32	6,80	0,97	0,00	0,00	0,00	0,00	0,00	0,00	0,00
Lanveur	L14	2,16	153,56	47,98	13,08	26,79	0,00	8,10	0,00	3,12	0,93	0,00	0,00	0,00	0,00	0,00	0,00	0,00
Lanveur	L15	2,20	154,95	48,33	13,67	24,67	0,00	9,33	1,00	1,33	1,67	0,00	0,00	0,00	0,00	0,00	0,00	0,00
Lanveur	L16	2,24	156,01	40,00	20,94	20,00	0,94	13,44	0,00	4,06	0,63	0,00	0,00	0,00	0,00	0,00	0,00	0,00
Lanveur	L17	2,34	159,06	42,12	18,01	19,94	0,96	18,01	0,00	0,96	0,00	0,00	0,00	0,00	0,00	0,00	0,00	0,00
Lanveur	L18	2,46	162,75	44,30	14,98	21,50	0,00	17,59	0,00	1,63	0,00	0,00	0,00	0,00	0,00	0,00	0,00	0,00
Lanveur	L19	2,59	166,70	28,71	11,88	11,55	0,00	36,30	0,33	9,90	1,32	0,00	0,00	0,00	0,00	0,00	0,00	0,00
Lanveur	L20	2,86	174,89	33,45	13,38	12,32	0,70	38,73	0,00	0,70	0,70	0,00	0,00	0,00	0,00	0,00	0,00	0,00
Lanveur	L21	2,94	177,10	38,79	14,23	10,68	1,42	34,88	0,00	0,00	0,00	0,00	0,00	0,00	0,00	0,00	0,00	0,00
Lanveur	L22	3,00	179,12	30,23	11,96	13,95	2,99	40,86	0,00	0,00	0,00	0,00	0,00	0,00	0,00	0,00	0,00	0,00
Lanveur	L23	3,19	184,83	30,23	11,63	10,30	3,99	42,52	0,33	0,33	0,66	0,00	0,00	0,00	0,00	0,00	0,00	0,00

Tresseny	T01	3,62	198,02	51,94	21,20	3,18	0,00	23,67	0,00	0,00	0,00	0,00	0,00	0,00	0,00	0,00	0,00	0,00
Tresseny	T02	3,61	197,72	63,57	16,43	0,00	0,00	20,00	0,00	0,00	0,00	0,00	0,00	0,00	0,00	0,00	0,00	0,00
Tresseny	T03	3,58	196,93	64,04	14,51	5,05	0,00	16,40	0,00	0,00	0,00	0,00	0,00	0,00	0,00	0,00	0,00	0,00
Tresseny	T04	3,57	196,38	42,33	16,67	1,33	0,00	39,67	0,00	0,00	0,00	0,00	0,00	0,00	0,00	0,00	0,00	0,00
Tresseny	T05	3,53	195,35	55,37	19,54	1,63	0,00	23,45	0,00	0,00	0,00	0,00	0,00	0,00	0,00	0,00	0,00	0,00
Tresseny	T06	3,51	194,59	55,24	19,23	2,10	0,00	23,43	0,00	0,00	0,00	0,00	0,00	0,00	0,00	0,00	0,00	0,00
Tresseny	T07	3,31	188,63	37,91	14,71	0,00	0,00	47,39	0,00	0,00	0,00	0,00	0,00	0,00	0,00	0,00	0,00	0,00
Tresseny	T08	3,26	187,05	34,13	17,75	0,00	0,00	48,12	0,00	0,00	0,00	0,00	0,00	0,00	0,00	0,00	0,00	0,00
Tresseny	T09	3,20	185,35	31,33	19,33	0,00	0,00	49,33	0,00	0,00	0,00	0,00	0,00	0,00	0,00	0,00	0,00	0,00
Tresseny	T10	3,12	182,77	32,45	15,89	0,00	0,00	51,66	0,00	0,00	0,00	0,00	0,00	0,00	0,00	0,00	0,00	0,00
Tresseny	T11	3,01	179,64	15,85	37,80	0,00	0,00	46,34	0,00	0,00	0,00	0,00	0,00	0,00	0,00	0,00	0,00	0,00
Tresseny	T12	2,97	178,21	13,10	40,34	0,00	1,72	44,83	0,00	0,00	0,00	0,00	0,00	0,00	0,00	0,00	0,00	0,00
Tresseny	T13	2,92	176,81	28,95	37,17	0,00	0,99	32,89	0,00	0,00	0,00	0,00	0,00	0,00	0,00	0,00	0,00	0,00
Tresseny	T14	2,72	170,79	4,88	3,66	0,00	0,00	58,54	25,00	6,71	0,61	0,61	0,00	0,00	0,61	0,00	0,00	0,00
Tresseny	T15	2,99	178,84	39,74	34,29	0,00	0,00	25,96	0,00	0,00	0,00	0,00	0,00	0,00	0,00	0,00	0,00	0,00
Tresseny	T16	2,99	178,88	26,85	42,28	1,01	0,00	26,17	1,68	0,00	2,01	0,00	0,00	0,00	0,00	0,00	0,00	0,00
Tresseny	T17	2,99	178,88	15,41	33,44	0,00	0,00	22,95	17,70	3,93	5,25	1,31	0,33	0,33	0,33	0,00	0,33	0,00
Tresseny	T18	2,75	171,49	5,77	19,87	0,32	0,00	20,19	32,05	4,81	13,46	3,53	0,64	0,64	0,96	0,00	0,00	1,28
Tresseny	T19	2,63	167,81	0,99	3,96	0,00	0,00	5,61	56,44	9,57	17,82	5,61	0,00	1,65	2,64	0,00	0,00	1,32
Tresseny	T20	2,55	165,41	0,00	0,00	0,00	0,00	0,00	64,09	13,76	15,44	6,71	1,01	1,68	2,68	0,00	0,00	1,34
Tresseny	T21	2,53	164,98	0,00	0,33	0,00	0,00	4,01	39,80	32,11	14,38	9,36	1,67	2,01	4,68	0,00	0,00	1,00
Tresseny	T22	2,51	164,32	0,00	0,64	0,00	0,00	0,00	69,77	15,76	8,68	5,14	0,64	1,29	2,57	0,00	0,00	0,64
Tresseny	T23	2,41	161,16	0,00	0,31	0,00	0,00	2,47	69,14	15,12	3,70	9,26	1,54	0,93	6,17	0,31	0,00	0,31
Tresseny	T24	2,30	158,05	0,62	0,93	0,62	0,00	1,24	68,32	15,53	0,00	12,73	1,86	1,86	8,07	0,31	0,00	0,62
Tresseny	T25	2,21	155,23	0,00	1,34	0,00	0,00	1,67	72,58	15,05	0,67	8,70	2,01	1,00	5,69	0,00	0,00	0,00
Tresseny	T26	2,08	151,34	0,31	0,31	0,00	0,00	3,74	65,11	13,40	5,92	11,21	3,12	1,87	4,05	0,31	0,62	1,25

Table S2. Relative total (dead and alive) abundances of foraminifera taxa found within the samples collected from the core P-C2 (Porzguen saltmarsh, bay of Brest).

Sample code	Elevation (m NGF)	Depth (m)	*Jadammina macrescens*	*Haplophragmoides wilberti*	*Trochammina inflata*	*Arenoparella mexicana*	*Miliammina fusca*	*Haynesina germanica*	*Elphidium sp.*	*Ammonia sp.*	Palaeomarsh elevation (m) from WA-PLS Model comp 3	RMSEP (m)	MinDC	MAT diagnostic	^{14}C a BP (see Table 2 for details)	mid sample elevation	RSL (m)	surface sampling error	core sampling error	Elevation error (benchmark & DGPS)	RMSEP (m)	Total error (m)
P-C2-E01	3,30;3,20	0,00;0.10	12,50	22,37	64,14	0,00	0,99	0,00	0,00	0,00	3,89	0,20	8,64	close		3,25	-0,64	0,10	0,05	0,13	0,20	0,48
P-C2-E02	3,20;3,10	0.10;0.20	39,47	3,95	54,28	1,32	0,99	0,00	0,00	0,00	3,70	0,20	14,78	close		3,15	-0,55	0,10	0,05	0,13	0,20	0,48
P-C2-E03	3,10;3,00	0.20;0.30	41,56	1,30	57,14	0,00	0,00	0,00	0,00	0,00	3,63	0,20	19,40	poor		3,05	-0,58	0,10	0,05	0,13	0,20	0,48
P-C2-E04	3,00;2,90	0.30;0.40	40,07	0,33	59,60	0,00	0,00	0,00	0,00	0,00	3,69	0,20	22,05	poor		2,95	-0,74	0,10	0,05	0,13	0,20	0,48
P-C2-E05	2,90;2,80	0.40;0.50	25,42	33,78	38,80	0,00	2,01	0,00	0,00	0,00	3,32	0,20	16,81	close		2,85	-0,47	0,10	0,05	0,13	0,20	0,48
P-C2-E06	2,80;2,70	0.50;0.60	21,85	2,46	74,77	0,62	0,31	0,00	0,00	0,00	4,13	0,20	20,41	poor		2,75	-1,38	0,10	0,05	0,13	0,20	0,48
P-C2-E07	2,70;2,60	0.60;0.70	21,78	2,31	74,92	0,66	0,33	0,00	0,00	0,00	4,14	0,20	20,60	poor		2,65	-1,49	0,10	0,05	0,13	0,20	0,48
P-C2-E08	2,60;2,50	0.70;0.80	32,40	0,80	66,00	0,40	0,40	0,00	0,00	0,00	3,89	0,20	20,11	poor		2,55	-1,34	0,10	0,05	0,13	0,20	0,48
P-C2-E09	2,50;2,40	0.80;0.90	50,90	1,20	47,31	0,00	0,60	0,00	0,00	0,00	3,39	0,20	12,37	close		2,45	-0,94	0,10	0,05	0,13	0,20	0,48
P-C2-E10	2,40;2,30	0.90;1.00	13,36	25,73	59,61	0,00	1,30	0,00	0,00	0,00	3,80	0,20	8,14	close		2,35	-1,44	0,10	0,05	0,13	0,20	0,48
P-C2-E11	2,30;2,20	1.00;1.10	15,83	10,07	73,02	0,00	1,08	0,00	0,00	0,00	4,07	0,20	13,37	close		2,25	-1,81	0,10	0,05	0,13	0,20	0,48
P-C2-E12	2,20;2,10	1.10;1.20	0,00	0,00	0,00	0,00	0,00	0,00	0,00	0,00	...	...	...	...		2,15	...	...	...	...	...	...
P-C2-E13	2,10;2,00	1.20;1.30	9,04	0,56	90,40	0,00	0,00	0,00	0,00	0,00	4,45	0,20	37,38	poor		2,05	-2,39	0,10	0,05	0,13	0,20	0,48
P-C2-E14	2,00;1,90	1.30;1.40	17,95	42,95	38,46	0,00	0,64	0,00	0,00	0,00	3,34	0,20	21,54	poor		1,95	-1,39	0,10	0,05	0,13	0,20	0,48
P-C2-E15	1,90;1,80	1.40;1.50	15,67	1,87	82,09	0,00	0,37	0,00	0,00	0,00	4,25	0,20	26,34	poor		1,85	-2,40	0,10	0,05	0,13	0,20	0,48
P-C2-E16	1,80;1,70	1.50;1.60	8,70	1,34	89,97	0,00	0,00	0,00	0,00	0,00	4,44	0,20	35,31	poor		1,75	-2,69	0,10	0,05	0,13	0,20	0,48
P-C2-E17	1,70;1,60	1.60;1.70	6,98	0,00	93,02	0,00	0,00	0,00	0,00	0,00	4,51	0,20	41,22	poor		1,65	-2,86	0,10	0,05	0,13	0,20	0,48
P-C2-E18	1,60;1,50	1.70;1.80	0,00	0,00	0,00	0,00	0,00	0,00	0,00	0,00	...	...	...	...		1,55	...	...	...	...	...	...
P-C2-E19	1,50;1,40	1.80;1.90	0,00	0,00	0,00	0,00	0,00	0,00	0,00	0,00	...	...	...	...		1,45	...	...	...	...	...	...
P-C2-E20	1,40;1,30	1.90;2.00	13,33	32,67	54,00	0,00	0,00	0,00	0,00	0,00	3,68	0,20	13,80	close		1,35	-2,33	0,10	0,05	0,13	0,20	0,48
P-C2-E21	1,30;1,20	2.00;2.10	10,85	1,55	87,60	0,00	0,00	0,00	0,00	0,00	4,38	0,20	33,18	poor		1,25	-3,13	0,10	0,05	0,13	0,20	0,48
P-C2-E22	1,20;1,10	2.10;2.20	34,42	40,06	25,52	0,00	0,00	0,00	0,00	0,00	3,01	0,20	26,14	poor		1,15	-1,85	0,10	0,05	0,13	0,20	0,48
P-C2-E23	1,10;1,00	2.20;2.30	37,11	5,84	57,04	0,00	0,00	0,00	0,00	0,00	3,65	0,20	17,02	close		1,05	-2,59	0,10	0,05	0,13	0,20	0,48
P-C2-E24	1,00;0,90	2.30;2.40	64,67	4,67	30,33	0,00	0,33	0,00	0,00	0,00	2,99	0,20	12,46	close		0,95	-2,03	0,10	0,05	0,13	0,20	0,48
P-C2-E25	0,90;0,80	2.40;2.50	60,26	2,61	34,53	0,00	2,61	0,00	0,00	0,00	3,10	0,20	5,85	close		0,85	-2,24	0,10	0,05	0,13	0,20	0,48
P-C2-E26	0,80;0,70	2.50;2.60	71,57	1,00	26,42	0,00	1,00	0,00	0,00	0,00	2,88	0,20	12,11	close		0,75	-2,13	0,10	0,05	0,13	0,20	0,48
P-C2-E27	0,70;0,60	2.60;2.70	67,01	0,34	32,31	0,00	0,34	0,00	0,00	0,00	3,02	0,20	12,85	close		0,65	-2,37	0,10	0,05	0,13	0,20	0,48
P-C2-E28	0,60;0,50	2.70;2.80	59,09	5,19	34,74	0,00	0,65	0,00	0,32	0,00	3,05	0,20	11,47	close		0,55	-2,50	0,10	0,05	0,13	0,20	0,48
P-C2-E29	0,50;0,40	2.80;2.90	54,55	2,60	42,21	0,32	0,32	0,00	0,00	0,00	3,30	0,20	11,82	close		0,45	-2,85	0,10	0,05	0,13	0,20	0,48
P-C2-E30	0,40;0,30	2.90;3.00	60,26	1,99	36,42	0,00	1,32	0,00	0,00	0,00	3,13	0,20	8,34	close		0,35	-2,78	0,10	0,05	0,13	0,20	0,48
P-C2-E31	0,30;0,20	3.00;3.10	45,08	5,08	49,15	0,34	0,34	0,00	0,00	0,00	3,49	0,20	14,67	close		0,25	-3,23	0,10	0,05	0,13	0,20	0,48
P-C2-E32	0,20;0,10	3.10;3.20	15,41	1,43	82,80	0,00	0,00	0,00	0,00	0,36	4,22	0,20	28,88	poor		0,15	-4,07	0,10	0,05	0,13	0,20	0,48
P-C2-E33	0,10;0,00	3.20;3.30	50,81	2,61	46,25	0,33	0,00	0,00	0,00	0,00	3,40	0,20	13,93	close		0,05	-3,35	0,10	0,05	0,13	0,20	0,48
P-C2-E34	0,00;-0,10	3.30;3.40	65,15	2,93	30,94	0,00	0,98	0,00	0,00	0,00	3,00	0,20	9,94	close		-0,05	-3,05	0,10	0,05	0,13	0,20	0,48
P-C2-E35	-0,10;-0,20	3.40;3.50	52,88	3,73	42,03	0,68	0,68	0,00	0,00	0,00	3,34	0,20	11,65	close	3500±60	-0,15	-3,49	0,10	0,05	0,13	0,20	0,48
P-C2-E36	-0,20;-0,30	3.50;3.60	40,60	3,69	54,03	0,34	1,34	0,00	0,00	0,00	3,61	0,20	14,35	close		-0,25	-3,86	0,10	0,05	0,13	0,20	0,48
P-C2-E37	-0,30;-0,40	3.60;3.70	17,75	29,01	51,27	0,00	1,97	0,00	0,00	0,00	3,61	0,20	8,67	close		-0,35	-3,96	0,10	0,05	0,13	0,20	0,48
P-C2-E38	-0,40;-0,50	3.70;3.80	63,14	4,44	32,08	0,00	0,34	0,00	0,00	0,00	3,03	0,20	11,94	close		-0,45	-3,48	0,10	0,05	0,13	0,20	0,48
P-C2-E39	-0,50;-0,60	3.80;3.90	63,31	5,19	26,62	0,65	4,22	0,00	0,00	0,00	2,99	0,20	5,60	close		-0,55	-3,54	0,10	0,05	0,13	0,20	0,48
P-C2-E40	-0,60;-0,70	3.90;4.00	53,82	1,27	41,08	1,27	2,55	0,00	0,00	0,00	3,38	0,20	7,77	close		-0,65	-4,03	0,10	0,05	0,13	0,20	0,48
P-C2-E41	-0,70;-0,80	4.00;4.10	56,56	6,25	34,38	0,31	2,50	0,00	0,00	0,00	3,14	0,20	8,17	close		-0,75	-3,89	0,10	0,05	0,13	0,20	0,48
P-C2-E42	-0,80;-0,90	4.10;4.20	51,22	5,23	42,51	0,35	0,70	0,00	0,00	0,00	3,33	0,20	12,31	close	4280±60	-0,85	-4,18	0,10	0,05	0,13	0,20	0,48
P-C2-E43	-0,90;-1,00	4.20;4.30	31,25	17,97	50,00	0,00	0,78	0,00	0,00	0,00	3,53	0,20	16,50	close		-0,95	-4,48	0,10	0,05	0,13	0,20	0,48
P-C2-E44	-1,00;-1,10	4.30;4.40	48,72	8,21	40,77	0,77	1,54	0,00	0,00	0,00	3,34	0,20	10,16	close		-1,05	-4,39	0,10	0,05	0,13	0,20	0,48
P-C2-E45	-1,10;-1,20	4.40;4.50	50,00	6,71	41,28	1,01	1,01	0,00	0,00	0,00	3,37	0,20	10,92	close		-1,15	-4,52	0,10	0,05	0,13	0,20	0,48
P-C2-E46	-1,20;-1,30	4.50;4.60	42,72	18,45	26,21	8,74	3,88	0,00	0,00	0,00	3,80	0,20	14,50	close		-1,25	-5,05	0,10	0,05	0,13	0,20	0,48
P-C2-E47	-1,30;-1,40	4.60;4.70	9,94	53,21	16,35	15,06	5,45	0,00	0,00	0,00	4,31	0,20	22,50	poor		-1,35	-5,66	0,10	0,05	0,13	0,20	0,48
P-C2-E48	-1,40;-1,50	4.70;4.80	9,97	27,24	62,79	0,00	0,00	0,00	0,00	0,00	3,87	0,20	12,51	close	4640±60	-1,45	-5,32	0,10	0,05	0,13	0,20	0,48
P-C2-E49	-1,50;-1,60	4.80;4.90	13,85	57,77	27,36	0,00	1,01	0,00	0,00	0,00	3,13	0,20	17,84	close		-1,55	-4,68	0,10	0,05	0,13	0,20	0,48
P-C2-E50	-1,60;-1,70	4.90;5.00	9,65	71,06	19,29	0,00	0,00	0,00	0,00	0,00	2,98	0,20	21,54	poor		-1,65	-4,63	0,10	0,05	0,13	0,20	0,48
P-C2-E51	-1,70;-1,80	5.00;5.10	3,21	75,36	19,64	1,07	0,71	0,00	0,00	0,00	3,11	0,20	21,01	poor	4775±60	-1,75	-4,86	0,10	0,05	0,13	0,20	0,48

Table S3. Relative total (dead and alive) abundances of foraminifera taxa found within the samples collected from the core T-C2 (Troaon saltmarsh, bay of Brest).

Sample code	Elevation (m NGF)	Depth (m)	*Jadammina macrescens*	*Haplophragmoides wilberti*	*Trochammina inflata*	*Arenoparella mexicana*	*Miliammina fusca*	*Haynesina germanica*	*Elphidium sp.*	*Ammonia sp.*	Palaeomarsh elevation (m) from WA-PLS Model comp 3	RMSEP (m)	MinDC	MAT diagnostic	^{14}C a BP (see Table 2 for details)	mid sample elevation	RSL (m)	surface sampling error	core sampling error	Elevation error (benchmark & DGPS)	RMSEP (m)	Total error (m)
Tr-C2-E01	3,40;3,30	0,00;0,10	7,42	49,03	24,84	0,32	18,39	0,00	0,00	0,00	3,18	0,20	0,27	good		3,35	0,17	0,10	0,05	0,13	0,20	0,48
Tr-C2-E02	3,30;3,20	0,10;0,20	38,49	2,30	24,34	0,00	34,87	0,00	0,00	0,00	3,05	0,20	13,81	close		3,25	0,20	0,10	0,05	0,13	0,20	0,48
Tr-C2-E03	3,20;3,10	0,20;0,30	47,74	2,58	31,61	0,00	18,06	0,00	0,00	0,00	3,12	0,20	2,07	good		3,15	0,03	0,10	0,05	0,13	0,20	0,48
Tr-C2-E04	3,10;3,00	0,30;0,40	59,87	8,41	28,80	0,65	2,27	0,00	0,00	0,00	3,04	0,20	9,39	close		3,05	0,01	0,10	0,05	0,13	0,20	0,48
Tr-C2-E05	3,00;2,90	0,40;0,50	58,86	2,85	33,54	0,63	4,11	0,00	0,00	0,00	3,14	0,20	4,31	close		2,95	-0,19	0,10	0,05	0,13	0,20	0,48
Tr-C2-E06	2,90;2,80	0,50;0,60	67,08	2,80	25,78	0,00	4,35	0,00	0,00	0,00	2,89	0,20	5,52	close		2,85	-0,04	0,10	0,05	0,13	0,20	0,48
Tr-C2-E07	2,80;2,70	0,60;0,70	54,97	2,32	39,74	0,00	2,98	0,00	0,00	0,00	3,23	0,20	5,44	close	940±56	2,75	-0,48	0,10	0,05	0,13	0,20	0,48
Tr-C2-E08	2,70;2,60	0,70;0,80	64,57	2,32	32,78	0,00	0,33	0,00	0,00	0,00	3,04	0,20	11,27	close		2,65	-0,39	0,10	0,05	0,13	0,20	0,48
Tr-C2-E09	2,60;2,50	0,80;0,90	66,77	3,23	29,03	0,00	0,97	0,00	0,00	0,00	2,95	0,20	10,57	close		2,55	-0,40	0,10	0,05	0,13	0,20	0,48
Tr-C2-E10	2,50;2,40	0,90;1,00	44,37	0,66	54,30	0,00	0,66	0,00	0,00	0,00	3,56	0,20	16,14	close		2,45	-1,11	0,10	0,05	0,13	0,20	0,48
Tr-C2-E11	2,40;2,30	1,00;1,10	59,43	1,26	38,68	0,00	0,63	0,00	0,00	0,00	3,18	0,20	10,36	close		2,35	-0,83	0,10	0,05	0,13	0,20	0,48
Tr-C2-E12	2,30;2,20	1,10;1,20	46,84	2,33	46,84	0,66	3,32	0,00	0,00	0,00	3,47	0,20	7,86	close		2,25	-1,22	0,10	0,05	0,13	0,20	0,48
Tr-C2-E13	2,20;2,10	1,20;1,30	54,19	1,61	43,23	0,00	0,97	0,00	0,00	0,00	3,30	0,20	10,04	close		2,15	-1,15	0,10	0,05	0,13	0,20	0,48
Tr-C2-E14	2,10;2,00	1,30;1,40	55,81	2,83	41,36	0,00	0,00	0,00	0,00	0,00	3,25	0,20	12,35	close		2,05	-1,20	0,10	0,05	0,13	0,20	0,48
Tr-C2-E15	2,00;1,90	1,40;1,50	55,02	3,56	41,42	0,00	0,00	0,00	0,00	0,00	3,25	0,20	12,64	close		1,95	-1,30	0,10	0,05	0,13	0,20	0,48
Tr-C2-E16	1,90;1,80	1,50;1,60	65,09	10,69	21,70	0,00	2,52	0,00	0,00	0,00	2,81	0,20	10,35	close		1,85	-0,96	0,10	0,05	0,13	0,20	0,48
Tr-C2-E17	1,80;1,70	1,60;1,70	49,35	3,57	47,08	0,00	0,00	0,00	0,00	0,00	3,39	0,20	14,34	close		1,75	-1,64	0,10	0,05	0,13	0,20	0,48
Tr-C2-E18	1,70;1,60	1,70;1,80	39,09	2,93	46,91	0,00	11,07	0,00	0,00	0,00	3,46	0,20	4,27	close		1,65	-1,81	0,10	0,05	0,13	0,20	0,48
Tr-C2-E19	1,60;1,50	1,80;1,90	62,74	2,55	34,71	0,00	0,00	0,00	0,00	0,00	3,09	0,20	12,02	close		1,55	-1,54	0,10	0,05	0,13	0,20	0,48
Tr-C2-E20	1,50;1,40	1,90;2,00	56,35	0,00	39,94	0,00	1,55	1,55	0,62	0,00	2,94	0,20	12,19	close		1,45	-1,49	0,10	0,05	0,13	0,20	0,48
Tr-C2-E21	1,40;1,30	2,00;2,10	59,03	0,00	39,68	0,00	0,00	1,29	0,00	0,00	3,05	0,20	15,35	close		1,35	-1,70	0,10	0,05	0,13	0,20	0,48
Tr-C2-E22	1,30;1,20	2,10;2,20	50,49	0,65	44,63	0,00	0,00	2,61	0,98	0,33	2,84	0,20	17,65	close		1,25	-1,59	0,10	0,05	0,13	0,20	0,48
Tr-C2-E23	1,20;1,10	2,20;2,30	52,46	0,00	44,06	0,00	1,45	0,00	2,03	0,00	3,01	0,20	13,15	close		1,15	-1,86	0,10	0,05	0,13	0,20	0,48
Tr-C2-E24	1,10;1,00	2,30;2,40	17,19	0,31	73,75	0,00	6,25	1,25	1,25	0,00	3,74	0,20	17,74	close		1,05	-2,69	0,10	0,05	0,13	0,20	0,48
Tr-C2-E25	1,00;0,90	2,40;2,50	57,19	2,81	33,75	0,00	5,63	0,00	0,63	0,00	3,00	0,20	2,74	good		0,95	-2,05	0,10	0,05	0,13	0,20	0,48
Tr-C2-E26	0,90;0,80	2,50;2,60	58,25	4,21	33,33	0,00	4,21	0,00	0,00	0,00	3,08	0,20	4,17	close		0,85	-2,23	0,10	0,05	0,13	0,20	0,48
Tr-C2-E27	0,80;0,70	2,60;2,70	45,45	3,03	40,00	0,00	3,64	3,33	4,55	0,00	2,16	0,20	12,77	close		0,75	-1,41	0,10	0,05	0,13	0,20	0,48
Tr-C2-E28	0,70;0,60	2,70;2,80	26,27	0,32	27,53	0,00	7,28	12,03	26,27	0,32	-0,49	0,20	32,27	poor		0,65	1,14	0,10	0,05	0,13	0,20	0,48
Tr-C2-E29	0,60;0,50	2,80;2,90	34,98	4,93	38,57	0,00	21,08	0,45	0,00	0,00	3,27	0,20	4,96	close		0,55	-2,72	0,10	0,05	0,13	0,20	0,48
Tr-C2-E30	0,50;0,40	2,90;3,00	38,59	6,04	47,65	0,00	2,68	3,36	1,68	0,00	2,79	0,20	15,54	close		0,45	-2,34	0,10	0,05	0,13	0,20	0,48
Tr-C2-E31	0,40;0,30	3,00;3,10	38,80	8,20	46,69	0,00	2,21	0,63	3,15	0,32	2,83	0,20	11,78	close		0,35	-2,48	0,10	0,05	0,13	0,20	0,48
Tr-C2-E32	0,30;0,20	3,10;3,20	26,05	1,61	41,16	0,00	6,43	10,61	13,83	0,32	-0,09	0,20	23,18	poor		0,25	0,34	0,10	0,05	0,13	0,20	0,48
Tr-C2-E33	0,20;0,10	3,20;3,30	8,77	0,00	10,06	0,00	0,32	50,65	25,32	4,87	-0,82	0,20	113,42	poor		0,15	0,97	0,10	0,05	0,13	0,20	0,48
Tr-C2-E34	0,10;0,00	3,30;3,40	22,13	0,00	44,68	0,00	4,68	14,04	11,49	2,98	-0,37	0,20	34,15	poor		0,05	0,42	0,10	0,05	0,13	0,20	0,48
Tr-C2-E35	0,00;-0,10	3,40;3,50	39,07	8,61	47,02	0,00	4,30	0,33	0,66	0,00	3,30	0,20	9,73	close	3690±70	-0,05	-3,35	0,10	0,05	0,13	0,20	0,48
Tr-C2-E36	-0,10;-0,20	3,50;3,60	38,82	7,57	51,32	0,00	0,99	0,66	0,66	0,00	3,34	0,20	15,99	close		-0,15	-3,49	0,10	0,05	0,13	0,20	0,48
Tr-C2-E37	-0,20;-0,30	3,60;3,70	33,01	8,74	55,02	0,65	1,29	0,65	0,65	0,00	3,51	0,20	13,86	close		-0,25	-3,76	0,10	0,05	0,13	0,20	0,48
Tr-C2-E38	-0,30;-0,40	3,70;3,80	9,45	34,53	46,91	8,14	0,98	0,00	0,00	0,00	4,30	0,20	20,27	poor	4230±60	-0,35	-4,65	0,10	0,05	0,13	0,20	0,48
Tr-C2-E39	-0,40;-0,50	3,80;3,90	3,63	48,84	41,91	4,95	0,33	0,00	0,33	0,00	3,87	0,20	21,98	poor		-0,45	-4,32	0,10	0,05	0,13	0,20	0,48
Tr-C2-E40	-0,50;-0,60	3,90;4,00	14,47	40,79	44,74	0,00	0,00	0,00	0,00	0,00	3,48	0,20	19,28	poor		-0,55	-4,03	0,10	0,05	0,13	0,20	0,48
Tr-C2-E41	-0,60;-0,70	4,00;4,10	40,55	14,33	42,68	0,91	1,52	0,00	0,00	0,00	3,43	0,20	13,77	close		-0,65	-4,08	0,10	0,05	0,13	0,20	0,48
Tr-C2-E42	-0,70;-0,80	4,10;4,20	42,04	11,46	45,22	0,00	1,27	0,00	0,00	0,00	3,39	0,20	14,24	close		-0,75	-4,14	0,10	0,05	0,13	0,20	0,48
Tr-C2-E43	-0,80;-0,90	4,20;4,30	0,00	0,00	0,00	0,00	0,00	0,00	0,00	0,00	...	...	...	...		...	...	...	...	...	...	...
Tr-C2-E44	-0,90;-1,00	4,30;4,40	0,00	0,00	0,00	0,00	0,00	0,00	0,00	0,00	...	...	...	...		...	...	...	...	...	...	...
Tr-C2-E45	-1,00;-1,10	4,40;4,50	3,85	11,54	84,62	0,00	0,00	0,00	0,00	0,00	4,35	0,20	23,41	poor		-1,05	-5,40	0,10	0,05	0,13	0,20	0,48
Tr-C2-E46	-1,10;-1,20	4,50;4,60	33,17	7,69	55,29	0,48	0,96	0,96	1,44	0,00	3,33	0,20	15,50	close		-1,15	-4,48	0,10	0,05	0,13	0,20	0,48
Tr-C2-E47	-1,20;-1,30	4,60;4,70	36,61	12,20	50,79	0,39	0,00	0,00	0,00	0,00	3,56	0,20	18,20	close		-1,25	-4,81	0,10	0,05	0,13	0,20	0,48
Tr-C2-E48	-1,30;-1,40	4,70;4,80	26,83	25,61	39,02	8,54	0,00	0,00	0,00	0,00	4,10	0,20	23,14	poor	4440±60	-1,35	-5,45	0,10	0,05	0,13	0,20	0,48
Tr-C2-E49	-1,40;-1,50	4,80;4,90	0,00	0,00	0,00	0,00	0,00	0,00	0,00	0,00	...	...	...	...		...	...	...	...	...	...	...
Tr-C2-E50	-1,50;-1,60	4,90;5,00	0,00	0,00	0,00	0,00	0,00	0,00	0,00	0,00	...	...	...	...		...	...	...	...	...	...	...
Tr-C2-E51	-1,60;-1,70	5,00;5,10	34,55	3,66	52,03	1,63	7,72	0,00	0,00	0,41	3,67	0,20	5,10	close	5450±70	-1,65	-5,32	0,10	0,05	0,13	0,20	0,48
Tr-C2-E52	-1,70;-1,80	5,10;5,20	15,02	24,46	41,63	12,45	0,86	3,43	2,15	0,00	3,82	0,20	27,87	poor		-1,75	-5,57	0,10	0,05	0,13	0,20	0,48
Tr-C2-E53	-1,80;-1,90	5,20;5,30	6,86	24,18	40,52	27,45	0,98	0,00	0,00	0,00	5,95	0,20	38,03	poor		-1,85	-7,80	0,10	0,05	0,13	0,20	0,48
Tr-C2-E54	-1,90;-2,00	5,30;5,40	10,57	56,10	29,27	0,81	3,25	0,00	0,00	0,00	3,26	0,20	11,21	close		-1,95	-5,21	0,10	0,05	0,13	0,20	0,48

Table S4. Relative total (dead and alive) abundances of foraminifera taxa found within the samples collected from the core A-C14 (Arun saltmarsh, bay of Brest).

Sample code	Elevation (m NGF)	Depth (m)	*Jadammina macrescens*	*Haplophragmoides wilberti*	*Trochammina inflata*	*Arenoparella mexicana*	*Miliammina fusca*	*Haynesina germanica*	*Elphidium sp.*	*Ammonia sp.*	Palaeomarsh elevation (m) from WA-PLS Model comp 3	RMSEP (m)	MinDC	MAT diagnostic	^{14}C a BP (see Table 2 for details)	mid sample elevation	RSL (m)	surface sampling error	core sampling error	Elevation error (benchmark & DGPS)	RMSEP (m)	Total error (m)
A-C14-E01	3,50;3,40	0.00;0.10	25,67	25,33	37,67	0,33	11,00	0,00	0,00	0,00	3,35	0,20	8,60	close		3,45	0,10	0,10	0,05	0,13	0,20	0,48
A-C14-E02	3,40;3,30	0.10;0.20	60,70	4,15	31,31	0,00	3,83	0,00	0,00	0,00	3,03	0,20	4,86	close		3,35	0,32	0,10	0,05	0,13	0,20	0,48
A-C14-E03	3,30;3,20	0.20;0.30	54,37	6,15	39,48	0,00	0,00	0,00	0,00	0,00	3,22	0,20	13,94	close		3,25	0,03	0,10	0,05	0,13	0,20	0,48
A-C14-E04	3,20;3,10	0.30;0.40	43,44	5,83	50,44	0,00	0,29	0,00	0,00	0,00	3,49	0,20	16,08	close		3,15	-0,34	0,10	0,05	0,13	0,20	0,48
A-C14-E05	3,10;3,00	0.40;0.50	50,84	3,68	45,48	0,00	0,00	0,00	0,00	0,00	3,35	0,20	13,80	close	436±55	3,05	-0,30	0,10	0,05	0,13	0,20	0,48
A-C14-E06	3,00;2,90	0.50;0.60	56,00	3,00	40,00	0,00	1,00	0,00	0,00	0,00	3,22	0,20	9,47	close		2,95	-0,27	0,10	0,05	0,13	0,20	0,48
A-C14-E07	2,90;2,80	0.60;0.70	60,00	2,00	37,00	0,00	1,00	0,00	0,00	0,00	3,15	0,20	9,11	close		2,85	-0,30	0,10	0,05	0,13	0,20	0,48
A-C14-E08	2,80;2,70	0.70;0.80	47,04	2,63	49,34	0,00	0,99	0,00	0,00	0,00	3,45	0,20	12,37	close		2,75	-0,70	0,10	0,05	0,13	0,20	0,48
A-C14-E09	2,70;2,60	0.80;0.90	34,62	1,60	63,78	0,00	0,00	0,00	0,00	0,00	3,80	0,20	20,11	poor		2,65	-1,15	0,10	0,05	0,13	0,20	0,48
A-C14-E10	2,60;2,50	0.90;1.00	30,68	0,00	69,32	0,00	0,00	0,00	0,00	0,00	3,93	0,20	24,20	poor		2,55	-1,38	0,10	0,05	0,13	0,20	0,48
A-C14-E11	2,50;2,40	1.00;1.10	37,00	1,00	64,00	0,00	0,00	0,00	0,00	0,00	3,77	0,20	21,82	poor		2,45	-1,32	0,10	0,05	0,13	0,20	0,48
A-C14-E12	2,40;2,30	1.10;1.20	34,00	2,00	62,00	0,00	0,00	0,00	0,00	0,00	3,79	0,20	19,07	poor		2,35	-1,44	0,10	0,05	0,13	0,20	0,48
A-C14-E13	2,30;2,20	1.20;1.30	36,43	2,75	60,82	0,00	0,00	0,00	0,00	0,00	3,73	0,20	18,65	poor		2,25	-1,48	0,10	0,05	0,13	0,20	0,48
A-C14-E14	2,20;2,10	1.30;1.40	39,68	0,00	60,32	0,00	0,00	0,00	0,00	0,00	3,71	0,20	23,33	poor		2,15	-1,56	0,10	0,05	0,13	0,20	0,48
A-C14-E15	2,10;2,00	1.40;1.50	67,33	0,33	32,34	0,00	0,00	0,00	0,00	0,00	3,02	0,20	13,92	close	1686±56	2,05	-0,97	0,10	0,05	0,13	0,20	0,48
A-C14-E16	2,00;1,90	1.50;1.60	39,93	9,24	50,83	0,00	0,00	0,00	0,00	0,00	3,51	0,20	18,23	close		1,95	-1,56	0,10	0,05	0,13	0,20	0,48
A-C14-E17	1,90;1,80	1.60;1.70	37,71	0,34	61,28	0,67	0,00	0,00	0,00	0,00	3,80	0,20	22,83	poor		1,85	-1,95	0,10	0,05	0,13	0,20	0,48
A-C14-E18	1,80;1,70	1.70;1.80	33,55	0,66	65,45	0,00	0,33	0,00	0,00	0,00	3,84	0,20	21,02	poor		1,75	-2,09	0,10	0,05	0,13	0,20	0,48
A-C14-E19	1,70;1,60	1.80;1.90	46,96	0,96	47,60	0,00	4,47	0,00	0,00	0,00	3,42	0,20	6,36	close		1,65	-1,77	0,10	0,05	0,13	0,20	0,48
A-C14-E20	1,60;1,50	1.90;2.00	62,25	0,00	28,81	0,00	8,94	0,00	0,00	0,00	2,99	0,20	3,14	good		1,55	-1,44	0,10	0,05	0,13	0,20	0,48
A-C14-E21	1,50;1,40	2.00;2.10	63,00	2,00	25,00	0,00	10,00	0,00	0,00	0,00	2,91	0,20	1,90	good		1,45	-1,46	0,10	0,05	0,13	0,20	0,48
A-C14-E22	1,40;1,30	2.10;2.20	65,57	2,40	19,76	0,00	12,28	0,00	0,00	0,00	2,79	0,20	4,57	close		1,35	-1,44	0,10	0,05	0,13	0,20	0,48
A-C14-E23	1,30;1,20	2.20;2.30	67,85	1,61	29,26	0,00	1,29	0,00	0,00	0,00	2,96	0,20	9,78	close		1,25	-1,71	0,10	0,05	0,13	0,20	0,48
A-C14-E24	1,20;1,10	2.30;2.40	42,57	3,30	52,81	0,00	1,32	0,00	0,00	0,00	3,54	0,20	14,02	close		1,15	-2,39	0,10	0,05	0,13	0,20	0,48
A-C14-E25	1,10;1,00	2.40;2.50	46,00	5,00	48,67	0,00	0,33	0,00	0,00	0,00	3,44	0,20	15,18	close		1,05	-2,39	0,10	0,05	0,13	0,20	0,48
A-C14-E26	1,00;0,90	2.50;2.60	44,73	5,43	45,05	0,00	4,79	0,00	0,00	0,00	3,38	0,20	6,18	close		0,95	-2,43	0,10	0,05	0,13	0,20	0,48
A-C14-E27	0,90;0,80	2.60;2.70	63,14	3,85	26,92	0,32	5,77	0,00	0,00	0,00	2,97	0,20	4,03	close		0,85	-2,12	0,10	0,05	0,13	0,20	0,48
A-C14-E28	0,80;0,70	2.70;2.80	58,86	2,01	29,43	0,00	9,70	0,00	0,00	0,00	3,02	0,20	0,54	good	2340±54	0,75	-2,27	0,10	0,05	0,13	0,20	0,48
A-C14-E29	0,70;0,60	2.80;2.90	57,24	2,41	38,62	0,00	1,72	0,00	0,00	0,00	3,19	0,20	7,56	close		0,65	-2,54	0,10	0,05	0,13	0,20	0,48
A-C14-E30	0,60;0,50	2.90;3.00	53,80	0,66	42,90	0,00	2,64	0,00	0,00	0,00	3,30	0,20	7,26	close		0,55	-2,75	0,10	0,05	0,13	0,20	0,48
A-C14-E31	0,50;0,40	3.00;3.10	56,72	3,61	36,07	0,00	3,61	0,00	0,00	0,00	3,15	0,20	4,60	close		0,45	-2,70	0,10	0,05	0,13	0,20	0,48
A-C14-E32	0,40;0,30	3.10;3.20	52,84	4,68	40,13	0,00	2,34	0,00	0,00	0,00	3,24	0,20	7,61	close		0,35	-2,89	0,10	0,05	0,13	0,20	0,48
A-C14-E33	0,30;0,20	3.20;3.30	67,23	3,38	28,72	0,68	0,00	0,00	0,00	0,00	3,01	0,20	14,05	close		0,25	-2,76	0,10	0,05	0,13	0,20	0,48
A-C14-E34	0,20;0,10	3.30;3.40	53,54	4,72	40,94	0,00	0,79	0,00	0,00	0,00	3,25	0,20	11,04	close		0,15	-3,10	0,10	0,05	0,13	0,20	0,48
A-C14-E35	0,10;0,00	3.40;3.50	53,77	2,05	36,99	0,00	1,37	3,42	2,40	0,00	2,39	0,20	13,76	close		0,05	-2,34	0,10	0,05	0,13	0,20	0,48
A-C14-E36	0,00;-0,10	3.50;3.60	50,17	1,67	47,49	0,00	0,67	0,00	0,00	0,00	3,40	0,20	12,13	close		-0,05	-3,45	0,10	0,05	0,13	0,20	0,48
A-C14-E37	-0,10;-0,20	3.60;3.70	41,58	1,98	47,52	0,00	3,96	3,96	0,99	0,00	2,81	0,20	12,61	close	2716±55	-0,15	-2,96	0,10	0,05	0,13	0,20	0,48

Table S5. Relative total (dead and alive) abundances of foraminifera taxa found within the samples collected from the core A-C10 (Arun saltmarsh, bay of Brest).

Sample code	Elevation (m NGF)	Depth (m)	*Jadammina macrescens*	*Haplophragmoides wilberti*	*Trochammina inflata*	*Arenoparella mexicana*	*Miliammina fusca*	*Haynesina germanica*	*Elphidium sp.*	*Ammonia sp.*	Palaeomarsh elevation (m) from WA-PLS Model comp 3	RMSEP (m)	MinDC	MAT diagnostic	^{14}C a BP (see Table 2 for details)	mid sample elevation	RSL (m)	surface sampling error	core sampling error	Elevation error (benchmark & DGPS)	RMSEP (m)	Total error (m)
A-C10-E01	3,52;3,42	0.00;0.10	40,58	39,29	7,79	0,00	12,34	0,00	0,00	0,00	2,65	0,20	16,24	close		3,47	0,82	0,10	0,05	0,13	0,20	0,48
A-C10-E02	3,42;3,32	0.10;0.20	51,16	6,31	39,87	0,00	2,66	0,00	0,00	0,00	3,24	0,20	8,26	close		3,37	0,13	0,10	0,05	0,13	0,20	0,48
A-C10-E03	3,32;3,22	0.20;0.30	66,56	2,68	29,10	0,00	1,67	0,00	0,00	0,00	2,96	0,20	8,77	close		3,27	0,31	0,10	0,05	0,13	0,20	0,48
A-C10-E04	3,22;3,12	0.30;0.40	65,15	1,95	32,57	0,00	0,33	0,00	0,00	0,00	3,03	0,20	11,37	close		3,17	0,14	0,10	0,05	0,13	0,20	0,48
A-C10-E05	3,12;3,02	0.40;0.50	53,80	3,63	42,57	0,00	0,00	0,00	0,00	0,00	3,28	0,20	12,92	close		3,07	-0,21	0,10	0,05	0,13	0,20	0,48
A-C10-E06	3,02;2,92	0.50;0.60	56,00	3,00	40,00	0,00	1,00	0,00	0,00	0,00	3,22	0,20	9,47	close		2,97	-0,25	0,10	0,05	0,13	0,20	0,48
A-C10-E07	2,92;2,82	0.60;0.70	60,26	1,60	37,50	0,00	0,64	0,00	0,00	0,00	3,15	0,20	10,13	close		2,87	-0,28	0,10	0,05	0,13	0,20	0,48
A-C10-E08	2,82;2,72	0.70;0.80	50,48	2,54	46,98	0,00	0,00	0,00	0,00	0,00	3,39	0,20	13,84	close		2,77	-0,62	0,10	0,05	0,13	0,20	0,48
A-C10-E09	2,72;2,62	0.80;0.90	52,67	2,33	45,00	0,00	0,00	0,00	0,00	0,00	3,34	0,20	13,11	close		2,67	-0,67	0,10	0,05	0,13	0,20	0,48
A-C10-E10	2,62;2,52	0.90;1.00	47,26	16,44	36,30	0,00	0,00	0,00	0,00	0,00	3,18	0,20	13,97	close	1081± 56	2,57	-0,61	0,10	0,05	0,13	0,20	0,48
A-C10-E11	1,72;1,62	1.80;1.90	47,03	15,35	37,62	0,00	0,00	0,00	0,00	0,00	3,21	0,20	14,16	close		1,67	-1,54	0,10	0,05	0,13	0,20	0,48
A-C10-E12	1,62;1,52	1.90;2.00	43,24	27,70	29,05	0,00	0,00	0,00	0,00	0,00	3,05	0,20	17,73	close		1,57	-1,48	0,10	0,05	0,13	0,20	0,48
A-C10-E13	1,52;1,42	2.00;2.10	61,00	8,00	22,00	0,00	9,00	0,00	0,00	0,00	2,85	0,20	4,34	close		1,47	-1,38	0,10	0,05	0,13	0,20	0,48
A-C10-E14	1,42;1,32	2.10;2.20	62,00	12,00	18,00	0,00	8,00	0,00	0,00	0,00	2,76	0,20	6,95	close		1,37	-1,39	0,10	0,05	0,13	0,20	0,48
A-C10-E15	1,32;1,22	2.20;2.30	66,00	9,00	25,00	0,00	0,00	0,00	0,00	0,00	2,87	0,20	15,82	close		1,27	-1,60	0,10	0,05	0,13	0,20	0,48
A-C10-E16	1,22;1,12	2.30;2.40	40,00	13,00	47,00	0,00	0,00	0,00	0,00	0,00	3,43	0,20	18,41	close		1,17	-2,26	0,10	0,05	0,13	0,20	0,48
A-C10-E17	1,12;1,02	2.40;2.50	47,48	15,97	36,55	0,00	0,00	0,00	0,00	0,00	3,18	0,20	13,94	close		1,07	-2,11	0,10	0,05	0,13	0,20	0,48
A-C10-E18	1,02;0,92	2.50;2.60	45,00	10,00	41,00	0,00	4,00	0,00	0,00	0,00	3,30	0,20	7,99	close		0,97	-2,33	0,10	0,05	0,13	0,20	0,48
A-C10-E19	0,92;0,82	2.60;2.70	62,00	6,00	25,00	0,00	7,00	0,00	0,00	0,00	2,90	0,20	4,51	close		0,87	-2,03	0,10	0,05	0,13	0,20	0,48
A-C10-E20	0,82;0,72	2.70;2.80	57,69	10,77	31,54	0,00	0,00	0,00	0,00	0,00	3,04	0,20	13,65	close		0,77	-2,27	0,10	0,05	0,13	0,20	0,48
A-C10-E21	0,72;0,62	2.80;2.90	62,96	7,78	29,26	0,00	0,00	0,00	0,00	0,00	2,97	0,20	15,61	close		0,67	-2,30	0,10	0,05	0,13	0,20	0,48
A-C10-E22	0,62;0,52	2.90;3.00	0,00	0,00	0,00	0,00	0,00	0,00	0,00	0,00	...	...	...	...		...	...	...	...	...	...	0,00
A-C10-E23	0,17;0,07	3.35;3.45	0,00	0,00	0,00	0,00	0,00	0,00	0,00	0,00	...	...	...	...		...	...	...	...	...	...	0,00
A-C10-E24	0,12;0,02	3.40;3.50	0,00	0,00	0,00	0,00	0,00	0,00	0,00	0,00	...	...	...	...		...	...	...	...	...	...	0,00
A-C10-E25	-0,28;-0,38	3.80;3.90	0,00	0,00	0,00	0,00	0,00	0,00	0,00	0,00	...	...	...	...		...	...	...	...	...	...	0,00

Table S6. Relative total (dead and alive) abundances of foraminifera taxa found within the samples collected from the core G-C2 (Tresseny saltmarsh).

Sample code	Elevation (m NGF)	Depth (m)	*Jadammina macrescens*	*Haplophragmoides wilberti*	*Trochammina inflata*	*Arenoparella mexicana*	*Miliammina fusca*	*Haynesina germanica*	*Elphidium sp.*	*Ammonia sp.*	*Lagena sulcata*	*Fissurina lucida*	*Quinqueloculina sp.*	*Favulina squamosa*	*Hopkinsina atlanticus*	*Bolivina variabilis*	Palaeomarsh elevation (m) from WA-PLS Model comp 2	RMSEP (m)	MinDC	MAT diagnostic	^{14}C a BP (see Table 2 for details)	mid sample elevation	RSL (m)	surface sampling error	core sampling error	Elevation error (benchmark & DGPS)	RMSEP (m)	Total error (m)
G-C2-E01	3.625;3.575	0.10;0.15	54,61	24,63	8,10	0,00	12,66	0,00	0,00	0,00	0,00	0,00	0,00	0,00	0,00	0,00	3,66	0,14	4,56	close		3,600	-0,059	0,10	0,025	0,12	0,14	0,39
G-C2-E02	3.525;3.475	0.20;0.25	60,52	22,37	10,14	0,00	6,97	0,00	0,00	0,00	0,00	0,00	0,00	0,00	0,00	0,00	3,79	0,14	7,29	close		3,500	-0,288	0,10	0,025	0,12	0,14	0,39
G-C2-E03	3.425;3.375	0.30;0.35	60,94	21,29	15,63	0,00	2,14	0,00	0,00	0,00	0,00	0,00	0,00	0,00	0,00	0,00	3,93	0,14	17,75	poor		3,400	-0,533	0,10	0,025	0,12	0,14	0,39
G-C2-E04	3.325;3.275	0.40;0.45	53,19	23,57	3,13	0,00	20,11	0,00	0,00	0,00	0,00	0,00	0,00	0,00	0,00	0,00	3,52	0,14	0,43	good		3,300	-0,218	0,10	0,025	0,12	0,14	0,39
G-C2-E05	3.225;3.175	0.50;0.55	46,23	16,11	4,62	0,00	33,04	0,00	0,00	0,00	0,00	0,00	0,00	0,00	0,00	0,00	3,48	0,14	2,60	good	431±28	3,200	-0,280	0,10	0,025	0,12	0,14	0,39
G-C2-E06	3.175;3.125	0.55;0.60	51,24	19,77	9,49	0,00	19,50	0,00	0,00	0,00	0,00	0,00	0,00	0,00	0,00	0,00	3,66	0,14	3,60	good		3,150	-0,509	0,10	0,025	0,12	0,14	0,39
G-C2-E07	3.125;3.075	0.60;0.65	57,90	20,08	8,84	0,00	13,18	0,00	0,00	0,00	0,00	0,00	0,00	0,00	0,00	0,00	3,73	0,14	2,59	good		3,100	-0,626	0,10	0,025	0,12	0,14	0,39
G-C2-E08	3.025;2.975	0.70;0.75	56,05	23,87	4,27	0,00	15,81	0,00	0,00	0,00	0,00	0,00	0,00	0,00	0,00	0,00	3,58	0,14	2,04	good		3,000	-0,582	0,10	0,025	0,12	0,14	0,39
G-C2-E09	2.925;2.875	0.80;0.85	54,12	21,33	6,20	0,00	18,35	0,00	0,00	0,00	0,00	0,00	0,00	0,00	0,00	0,00	3,61	0,14	1,69	good		2,900	-0,710	0,10	0,025	0,12	0,14	0,39
G-C2-E10	2.825;2.775	0.90;0.95	52,86	22,08	5,05	0,00	20,01	0,00	0,00	0,00	0,00	0,00	0,00	0,00	0,00	0,00	3,56	0,14	0,76	good		2,800	-0,764	0,10	0,025	0,12	0,14	0,39